



저작자표시-비영리-변경금지 2.0 대한민국

이용자는 아래의 조건을 따르는 경우에 한하여 자유롭게

- 이 저작물을 복제, 배포, 전송, 전시, 공연 및 방송할 수 있습니다.

다음과 같은 조건을 따라야 합니다:



저작자표시. 귀하는 원저작자를 표시하여야 합니다.



비영리. 귀하는 이 저작물을 영리 목적으로 이용할 수 없습니다.



변경금지. 귀하는 이 저작물을 개작, 변형 또는 가공할 수 없습니다.

- 귀하는, 이 저작물의 재이용이나 배포의 경우, 이 저작물에 적용된 이용허락조건을 명확하게 나타내어야 합니다.
- 저작권자로부터 별도의 허가를 받으면 이러한 조건들은 적용되지 않습니다.

저작권법에 따른 이용자의 권리는 위의 내용에 의하여 영향을 받지 않습니다.

이것은 [이용허락규약\(Legal Code\)](#)을 이해하기 쉽게 요약한 것입니다.

[Disclaimer](#)

공학석사 학위논문

A study on the effect of the impressed
current cathodic protection system in
reinforced concrete structures

철근 콘크리트 구조물에 적용되는 외부전원식
음극방식 효과에 관한 연구



2018년 8월

한국해양대학교 대학원

기관시스템공학과

고 권 흠

본 논문을 고권흙의 공학석사
학위논문으로 인준함.

위원장 이 상 득
위원 오 세 진
위원 정 진 아



2018년 6월 27일

한국해양대학교 대학원
기관시스템공학과

고 권 흙

TABLE OF CONTENTS

Table of contents	i
List of tables	iii
List of figures	iv
Abstract	vii
Chapter 1 INTRODUCTION	1
Chapter 2 BACKGROUND	4
2.1 Corrosion basics	4
2.1.1 Definition of corrosion	4
2.1.2 Thermodynamic and electrode potential	6
2.1.3 Electrochemical reactions in aqueous	11
2.1.4 Polarization	13
2.1.5 Passivity	18
2.2 Corrosion of steel in reinforced concrete	21
2.3 Corrosion of steel by chloride in reinforced concrete	24
2.4 Cathodic protection of reinforced concrete	26
2.4.1 Sacrificial Anode Cathodic Protection (SACP)	26
2.4.2 Impressed Current Cathodic Protection (ICCP)	29
Chapter 3 LITERATURE REVIEW	31
3.1 Availability of cathodic protection in reinforced concrete	31
3.2 Effect of CP in chloride environment	35
3.3 Arrangement and type of anode for ICCP in RC	39

Chapter 4 EXPERIMENTAL PROCEDURES	45
4.1 Specimens	45
4.2 Manufacture of anodes for ICCP and installation	48
4.3 Installation of test devices	50
4.4 Procedures & analysis	53
4.4.1 Measurement of E–log i on the specimens	53
4.4.2 Measurement of cathodic protection potential	55
4.4.3 Measurement of depolarization potential	56
4.4.4 Measurement of cathodic protection current	57
Chapter 5 RESULTS & DISCUSSION	58
5.1 Results of measuring E–log i on the beam type specimens	58
5.2 Results of measuring cathodic protection potential	60
5.3 Results of measuring depolarization potential on the beam type specimens	62
5.4 Results of measuring depolarization potential on the slab type specimens	66
5.5 Results of measuring cathodic protection current	70
Chapter 6 CONCLUSION	73
Reference	76

List of Tables

Table 2.1 Potential value for common secondary reference electrodes	10
Table 3.1 Results of test for the potential of reinforcing steels	33
Table 3.2 The measurement of polarization after switching off	37
Table 3.3 Corrosion rate at the low corrosion level	41
Table 3.4 Bond stress, slip and % mass loss at the whole corrosion level	41
Table 3.5 The compression capacity and deformation of column	43
Table 3.6 Measurement results of initial half cell potential and corrosion rate	43
Table 3.7 Ratio of the average value of current within each layer of rebars for specimens with different concrete resistivity	44
Table 3.8 Ratio of the average value of current within each layer rebars for specimens with different impressed current density	44
Table 4.1 Detail contents of the reinforced concrete specimen	46

List of Figures

Fig. 2.1 Corrosion reaction of iron in the nature	5
Fig. 2.2 Schematic diagram of electric double layer	9
Fig. 2.3 Pourbaix diagram for the iron	9
Fig. 2.4 Electrochemical reaction in HCl solution	12
Fig. 2.5 Activation overvoltage tend to Tafel's region	17
Fig. 2.6 Schematic polarization behavior	20
Fig. 2.7 Pourbaix diagram for the iron in the concrete	23
Fig. 2.8 Pitting corrosion after being broken passive layer by chloride content	25
Fig. 2.9 E–pH diagram for the iron in chloride environment	25
Fig. 2.10 The sacrificial anode cathodic protection system	28
Fig. 2.11 Typical polarization curve in SACP	28
Fig. 2.12 Impressed current cathodic protection system	30
Fig. 2.13 Typical polarization in ICCP	30
Fig. 3.1 Corrosion rates summary from polarization resistance test ...	33
Fig. 3.2 Time–dependent corrosion rate of RC structures during the whole life–cycle	34
Fig. 3.3 The depolarization test compared the cathodic protection and cathodic prevention	37
Fig. 3.4 Comparison between throwing power of potential obtained from the numerical models	38

Fig. 3.5	Potential distribution of steel in concrete (a) without chlorides and (b) with 3% chloride by weight of cement during a depolarization test carried out after 24 months of CP application	38
Fig. 3.6	The polarization curve of 50% pumice mortar containing 0.7% CF	42
Fig. 3.7	The potential of all specimens during the test	42
Fig. 4.1	Beam type specimen	46
Fig. 4.2	Slab type specimen	47
Fig. 4.3	Installation of 3 types of anode in the beam type specimens	49
Fig. 4.4	Anode of Ribbon and Mesh type grouted by mortar	49
Fig. 4.5	Installation of 3 types of anode in slab type specimens	49
Fig. 4.6	Picture of cathodic protection test on the beam type concrete specimens	51
Fig. 4.7	Picture of cathodic protection test on the slab type concrete specimens	51
Fig. 4.8	Schematic diagram of beam type specimen installed anode and reference electrode for cathodic protection	52
Fig. 4.9	Schematic diagram of slab type specimen installed anode and reference electrodes for cathodic protection	52
Fig. 4.10	Schematic diagram for electrochemical polarization test	54
Fig. 5.1	E-log i graph for the beam type specimen	59
Fig. 5.2	Protection potential on the beam type specimen with diverse anodes by different environments	59
Fig. 5.3	The cathodic protection potential in experimental environments	61
Fig. 5.4	Potential shift variation of beam specimen with Ti-Ribbon anode during an instant-off measurement of ohmic interference	64

Fig. 5.5 Potential shift variation of beam specimen with Ti-Rod anode during an instant-off measurement of ohmic interference	64
Fig. 5.6 Potential shift variation of beam specimen with Ti-Mesh anode during an instant-off measurement of ohmic interference	65
Fig. 5.7 Potential shift variation of slab specimen with a Ti-Ribbon anode during an instant-off measurement of ohmic interference at 3% sea water condition	68
Fig. 5.8 Potential shift variation of slab specimen with a Ti-Ribbon anode and a Ti-Rod anode during an instant-off measurement of ohmic interference at 3% sea water condition	68
Fig. 5.9 Potential shift variation of slab specimen with a Ti-Ribbon anode and a Ti-Mesh anode during an instant-off measurement of ohmic interference at 3% sea water condition	69
Fig. 5.10 Protection current on the specimens with diverse anodes in sea water	71
Fig. 5.11 Protection current on the specimens with diverse anodes in fresh water	71
Fig. 5.12 Protection current on the specimens with diverse anodes in air	72

A study on the effect of the impressed current cathodic protection system in reinforced concrete structures

KO, KWONHEUM

Department of Marine System Engineering
Graduate School of Korea Maritime and Ocean University

Abstract

Reinforced concrete has been used as a construction material at variable fields related to our life such as air port, bridge, and ocean concrete structure, etc. The rebar in the concrete is protected from the corrosion because the passive layer is formed by high alkaline environment. Over the time, however, the rebar in the concrete is prone to corrode according to the corrosive environment and the structure of the concrete building. For example, the chloride ion plays a key role in corrosion process because it breaks the passive layer on the rebar and accelerates the corrosion rate. Besides, the volume of rebar is increased by the consequence of corrosion and then the concrete is spalled simultaneously.

The cathodic protection was invented and used widely to protect rebars in the reinforced concrete structure against the corrosion. Additionally, The cathodic protection is divided to Sacrificial Anode Cathodic Protection (SACP) and Impressed Current Cathodic Protection (ICCP). Although ICCP system is expensive to install initially and is complex, this is applied more

frequently to impede the corrosion in reinforced concrete structure than SACP. It explains roughly; ICCP supplies the protection current from the anode to the cathode (rebar) and then it prevents the corrosion of rebar and delays the corrosion rate.

In complex RC structure, there are limitations on SACP system such as concrete resistivity, throwing power of CP and experimental environment, so it is difficult to expect to protect perfectly. Therefore, it needs to investigate the major factors having effect on the whole protection in complex structure of the building. However, ICCP is exploited as a practical way primarily to protect the corrosion of rebar in the concrete these days.

For this study, the anode such as Ti-Mesh, Ti-Rod and Ti-Ribbon was installed on the reinforced concrete specimen of beam and slab type. In addition, the electrochemical test was conducted to confirm the cathodic protection performance depending to the exposed environment and the kind of anode in RC structure applied with ICCP ; E-log i, cathodic protection potential, depolarization, cathodic protection current.

The following results have been obtained through the present study about the cathodic protection efficiency :

1) The E-log i test was conducted to affirm the standard of cathodic protection potential on the beam type specimen according to the environment. The standard value of cathodic protection potential was measured to about 90 ~ 140 mV. Besides, the value depending on the corrosive environment was inclined to increase slightly in order of atmosphere, fresh water and 3% NaCl solution. However, the kind of anode for ICCP nearly had no effect on the cathodic protection efficiency.

2) The cathodic protection potential was gauged by the galvanicstatic

method on the beam type specimen applied with ICCP. The shape of anode had not major effect on the behavior of cathodic protection potential. In addition, the value of protection potential was tended to decrease in order of atmosphere, fresh water and 3% NaCl solution and then it was trivial difference between them.

3) The cathodic protection current was measured by the potentiostatic method after applying with ICCP on the beam type specimen and the degree of cathodic protection current was increased by all anodes in order of atmosphere, fresh water and 3% NaCl solution.

4) The degree of depolarization was investigated on beam type specimen. The IR-Drop was the highest in atmosphere because of the concrete resistivity. On the other hand, it was the lowest in the 3% NaCl solution. Moreover, when the corrosiveness of experimental environment was higher (more severe), the real degree of depolarization except IR-Drop was more increased by concrete resistivity.

5) The cathodic protection potential was evaluated on the slab type specimen. When the distance from the anode to the rebar (cathode) is closer, the protection potential was lower by the concrete resistivity. Additionally, the potential difference represented proportionally 50 mV per 60 mm which was the distance between rebars.

6) In protecting the slab type specimen by ICCP, as the distance between the location of rebar and the anode was farther, the concrete resistivity was increased more and then the supply of protection current was limited. However, after installing the anode at regular distance supplementarily, the unprotected rebar was enabled to protect well totally.

7) As the results of protecting the slab type specimen by ICCP, it would be able to find the maximum protection distance which is about 150

mm to the rebar from the anode. That is, the anode should be installed at interval of about 300 mm to protect the whole rebars uniformly without the unprotected area.

It was found through the above results that the shape of anode used by ICCP had insignificant effect on the protection efficiency. The protection efficiency of ICCP was changed in accordance with the spacing between the anode and rebar, and the location of anode. So, it should consider those points throughly in designing the impressed current cathodic protection. In addition, when the proper cathodic protection is applied to the reinforced concrete structures, the enormous economic problems by the corrosion will be resolved as well as the safety for human life.



초록

철근 콘크리트는 건축 재료로서 우리의 삶과 연관된 공항, 교량, 해양 구조물 등 다양한 분야에서 사용하고 있다. 콘크리트 내부에 있는 철근의 경우, 콘크리트 특유의 고 알칼리성 환경으로 인해 철근 표면에 부동태 피막을 형성한다. 그러므로 부식을 피할 수 있게 된다. 그러나 시간이 경과하면서 부식성 환경과 건물의 복잡한 구조에 따라 철근은 쉽게 부식된다. 예를 들면, 염소 이온은 철근 표면의 부동태 피막을 파괴하고 부식속도를 가속화하는 주요한 부식성 요소이다. 게다가, 부식에 의해 철근의 부패가 증가하고, 동시에 콘크리트의 부서짐 및 탈락현상이 발생한다.

철근 콘크리트 구조물의 방식을 위해 음극방식법이 개발되었고, 널리 사용되고 있다. 게다가, 음극 방식법은 희생양극식과 외부전원식으로 나뉜다. 비록 외부전원식 음극방식법은 초기 설치 비용이 많이 들며 구조가 복잡하지만, 철근 콘크리트 구조물의 경우 희생양극식 음극방식법보다 주로 사용되고 있다. 외부전원식 음극 방식법을 간략히 설명하면 시스템 내의 음극과 양극 사이에 방식 전류를 공급하여 방식을 시행하고 방식 속도를 늦춰주는 역할을 한다.

복잡한 구조의 철근 콘크리트의 경우, 희생양극식 음극 방식법은 콘크리트 비저항, 음극방식 시스템의 전달력 그리고 실험 환경 등의 방해 요소에 의해 완벽한 방식을 기대하기 어렵다. 따라서 복잡한 구조로 된 건물의 전체적인 방식에 영향을 주는 요소들을 조사할 필요가 있다. 그러나 외부전원식 음극방식법은 콘크리트 내부의 철근을 방식하기 위하여 오늘날에 사용하고 있는 가장 적절한 방법이다.

본 연구에서 Ti-Mesh, Ti-Rod, Ti-Ribbon 양극을 보(Beam) 및 슬랩(Slab) 형식의 철근콘크리트 시험편에 설치하였다. 그리고 외부전원법이 적용된 철근콘크리트 구조물의 노출환경 및 양극의 종류에 따른 음극방식성능을 확인하기 위하여 E-log i, 음극방식전위, 복극 그리고 음극 방식 전류와 같은

전기화학적 실험을 실행한 결과 다음과 같은 결론을 얻었다.

1) 보 시험편에 대한 환경별 음극방식 전위 기준을 확인하기 위한 방법으로 E-log i 측정 실험을 시행한 결과, 음극방식 전위기준 값은 약 90~140 mV로 측정되었다. 또한 부식 환경별로 음극방식 전위기준 값은 공기, 청수, 해수 순으로 약간 증가하는 경향이 나타났으나 양극의 종류와는 거의 무관한 결과를 나타내었다.

2) 정전류법으로 보 시험편에 음극방식을 적용한 후 방식전위 측정 결과 양극의 종류는 방식전위거동에 큰 영향을 미치지 않았으며, 부식 환경별로는 공기, 청수, 해수 순으로 방식전위 값이 낮아지는 경향이 나타났으나 그 차이는 크지 않았다.

3) 정전위법으로 보 시험편에 음극방식을 적용한 후 방식전류 측정결과 3종의 양극 모두 공기, 청수, 해수 순으로 방식전류량이 증가하였다.

4) 보 시험편에서 복극량을 측정한 결과, 콘크리트 비저항에 의한 전압강하가 공기 중에서 가장 큰 값을 나타냈고, 3% 염수 환경에서 가장 낮게 나타났다. 또한 부식성 환경이 가혹할수록 비저항에 의한 전압강하를 배제한 순수한 복극량이 더욱 증가함을 확인할 수 있었다.

5) 슬랩 시험편의 방식전위 측정결과, 콘크리트 비저항으로 인하여 철근의 위치가 양극에서 가까울수록 방식전위가 낮아지는 것을 확인할 수 있었으며, 철근이 배근된 간격 60 mm당 약 50 mV씩 비례적으로 전위차가 발생하였다.

6) 슬랩 시험편을 외부전원법으로 방식할 경우, 철근의 위치가 양극과 멀어질수록 콘크리트의 비저항이 증가하여 방식전류의 공급이 제한되었으나 일정 간격으로 양극을 추가적으로 설치함으로써 미방식되었던 철근까지 방식할 수 있었다.

7) 슬랩 시험편을 외부전원법으로 방식한 결과, 양극이 설치된 위치에서 약 150 mm 떨어진 철근까지 방식할 수 있었다. 즉, 미방식되는 영역이 없이 전체의 시험편을 균일하게 방식하기 위해서는 양극을 약 300 mm 간격으로 설치해

야 한다.

이상의 결과를 통해 외부전원식 음극방식에 사용되는 양극의 형상은 방식 성능에 큰 영향을 미치지 않음을 확인할 수 있었다. 또한 외부전원법은 양극과 철근과의 배치간격 및 양극의 설치위치에 의해 방식성능이 달라지기 때문에 외부전원식 음극방식 설계 시 이를 충분히 고려해야 한다. 게다가, 철근 콘크리트 구조물에 적절한 음극방식을 적용하면 막대한 경제적인 문제뿐만 아니라 인명 안전 문제를 해결할 수 있으리라 사료된다.



Chapter 1

INTRODUCTION

Reinforced concrete is used as a complex construction material at variable fields related to our life such as air port, bridge, and ocean concrete structure, etc. Rebar also is a great material with durability, fire resistance and tensile strength against external force. In case of concrete, it has high resistivity and especially forms high-alkaline environment with water. The rebars can be prevented from the corrosion in high alkaline environment because passive layer is formed[8]. As mentioned earlier, the reinforced concrete had been thought the best construction material because the concrete and rebar respectively complement each other.

If the alkaline environment is changed to neutral or acid by containing abnormal factors, however, the corrosion of rebar occurs[10, 16, 20, 26]. Moreover, the passive layer on the rebar is broken by chloride contents, which are leading to severe pitting corrosion. In general corrosion of the concrete, the volume of corrosive products is increased and the concrete is spalled partially[5]. The crack on the concrete allows corrosive environment factors such as oxygen, water and others to invade easily and accelerate the corrosion rate.

When making design of structure, service life of the building is determined and then it is built by the confirmed plan. However, the service life of the building is reduced more strikingly in harsh corrosive environment than the planned life. So, the repair of the building has been needed to maintain the service life to the planned lifetime. Therefore, this status makes enormous economic problem as well as safety problem of human life[24].

The economic impact of corrosion was investigated by NACE from 1999 to 2001 in the United States. The results of the study show the total estimated direct cost of corrosion is approximately \$276 billion which is about 3.1% of the nation's gross domestic product (GDP). In addition, annual direct cost of the bridge and highway, one of industry categories, estimates \$8.3 billion. The indirect costs also were estimated approximately to be as high as 10 times that of direct corrosion costs [29].

Leo Frigo Memorial Bridge failure occurred in Sep 24th 2013, the United States because the pilings nearby piers had been corroded. Moreover, the bridge was closed for three months and a half for repairs and then the estimated effect of closing the bridge was approximately \$14.5 million [30].

Lowe's Motor Speedway Bridge collapse happened in US on May 20th 2000. The cause of that was identified due to corrosion of steel supports. In addition, many people were injured severely by the bridge failure [31].

These days, diverse methods such as ICCP and SACP are being invented and studied to protect from the corrosion in the concrete structures and steel products [11, 14, 21].

In using SACP, sacrificial anode is formed the passive layer on the surface in high alkaline environment, which is result in insufficient effect. Moreover, the corrosion problem generates severely because the protection current may not be supplied to the cathode (rebar). Therefore, when using the SACP, this phenomenon should be considered to hinder the corrosion in the high alkaline environment. In the impressed current cathodic protection, the efficiency for the protection is lowered due to interference effect by leakage current. Moreover, the reinforced concrete is heterogeneous and also has high

resistivity. Considered those, the ICCP supplying DC current forcedly according to the condition of rebar is more useful than the SACP using the metal ionization.

When evaluating the cathodic protection efficiency of ICCP, various factors, arrangement of rebars, concrete–water ratio, type and arrangement of insoluble anode and exposed condition of RC, etc, should be investigated for the uniform protection of the whole structure by applying ICCP.

The purpose of this study was to find the proper ICCP method in the complex structure where it is difficult to install the anodes. For instance, when using one anode, it is less likely to protect from the corrosion of rebars totally in complicated structure because the above factors such as the experimental environment and the type of anode disturb the cathodic protection. Moreover, if the particular anode can not be installed in the complicated structure, it results in the severe corrosion.

In this study, the anode for ICCP was exploited as different shape such as Ti–Rod, Ti–Mesh and Ti–Ribbon and then was mounted on the concrete specimen. In addition, the electrochemical test as follows was carried out to find the optimal cathodic protection efficiency on various specimens according to the experimental environments. it was E–log i, cathodic protection potential, depolarization potential and cathodic protection current.

Chapter 2

BACKGROUND

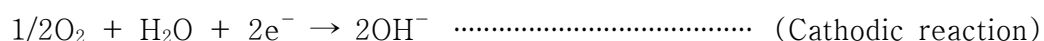
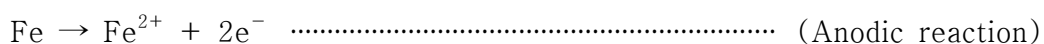
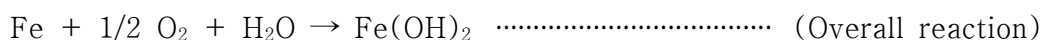
2.1 Corrosion basic

2.1.1 Definitions of corrosion

Corrosion is the chemical reactions between a metal and environmental factors. That is, the metal becomes metallic ions by dissolving. In addition, corrosion is the destructive results of chemical reactions between metal or alloy and their environments[27]. If the machinery and equipment are composed with metal or alloy in the plant, those finally will be out of order since it can't operate normally.

The electrochemical reactions are a total chemical reaction in a metal corrosion which is movement of electrons on their electrodes. when occurring corrosion reactions, the electrodes are divided by the electrons to negative(cathode) and positive(anode). Moreover, the negative electrode mostly is environment factors because it get electrons from the other. on the other hand, the metal is to be positive by losing the electrons. The corrosion reaction of iron simply is represented by Figure 2.1.

The corrosion reaction of iron in nature briefly shows as follows ;



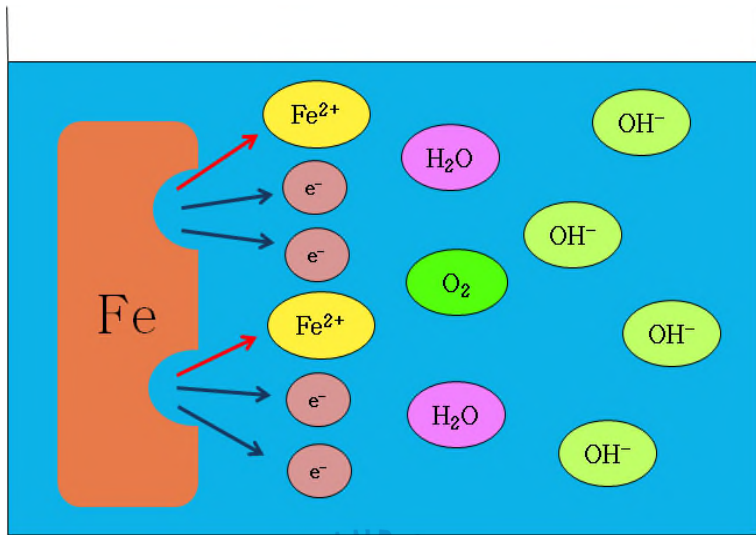


Figure 2.1 Corrosion reaction of iron in the nature



2.1.2 Thermodynamics and electrode potential

Corrosion in aqueous solution is made up of the electrons shift. The rate of corrosion reaction is affected by a change in electrochemical potential or the electron activity or availability at a metal surface[27]. Therefore, the corrosion reaction is called electrochemical reaction generally.

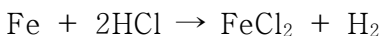
Thermodynamics gives information about the energy change in corrosion reaction. This energy change indicates the condition of corrosion and serves as driving force. In addition, thermodynamics shows whether or not it is possible to occur the reaction of corrosion. However, this cannot expect and decide the rate of corrosion.

In case there is a conducting metal in aqueous solution, polar H₂O molecules are attracted to the conductive metallic surface[27]. The outer Helmholtz plane is formed by this phenomenon and plays a role like a charged capacitor because of having the electrical double layer, as indicated in Figure 2.2.

1) Free energy

Thermodynamic considerations in electrochemistry give information which can decide whether or not a reaction will be able to occur spontaneously without external energy. All processes which occur spontaneously have a Gibbs free energy change (ΔG) related to those is negative shown as Figure 2.3.

The corrosion of iron in hydrochloric acid shows that:



The above reaction shows a change of free energy(ΔG).

Free energy change(ΔG) is associated with electrochemical potential(E) and represent as follows:

$$\Delta G = -nFE$$

n : the number of exchanged equivalents in reaction

F : Faraday's constant (96,500 Coulomb/equiv.)

E : the electric potential

Through the above formula,

$\Delta G > 0$; cathodic reduction reaction on metal

$\Delta G = 0$; at equilibrium

$\Delta G < 0$; anodic oxidation reaction on metal

2) Reference electrode

When electrochemical reaction occurs, equilibrium potential can be indicated through Nernst equation :



$$E = E^\circ + \frac{RT}{nF} \ln \frac{[\text{Ox}]}{[\text{Red}]}$$

n : the number of exchanged equivalents in reaction

R : gas constant (8.314J/deg·mol)

F : Faraday's constant (96,500 coulomb/equiv.)

T : Kelvin temperature

$[\text{OX}]$: concentration or activity of oxidize

$[\text{Red}]$: concentration or activity of reduced substance

E° : equilibrium potential (standard electrode potential)

at $[OX]=1$, $[Red]=1$

The equilibrium potential of half-cell metal can be calculated promptly by the above equation but absolute value of this can not do. This is because the differential values are represented by the standard solution. Hence, potential value gained by the calculation is not a absolute value and is difference value between electrodes.

As this reasons, the reference electrode is needed to measure potential value, which must be recorded after measuring on the paper. There are most popular electrodes such as ; Standard Hydrogen Electrode(SHE), Saturated Silver-Silver chloride Electrode(SSCE), Saturated Calomel Electrode(SCE), Copper-Copper Sulphate Electrode(CSE), etc. Table 2.1 represents the kind and compared potential of reference electrodes.

3) Pourbaix Diagram

Pourbaix diagram is created by Ph. Marcel Pourbaix, which indicates the condition of corrosion on pH-potential graph. the potential values calculated by Nernst equation are recorded the condition of metals in acid, neutral or alkaline environment. In addition, depending on the state of the metal in each environment, it is divided into areas of corrosion, passivity and immunity as shown in Figure 2.3.

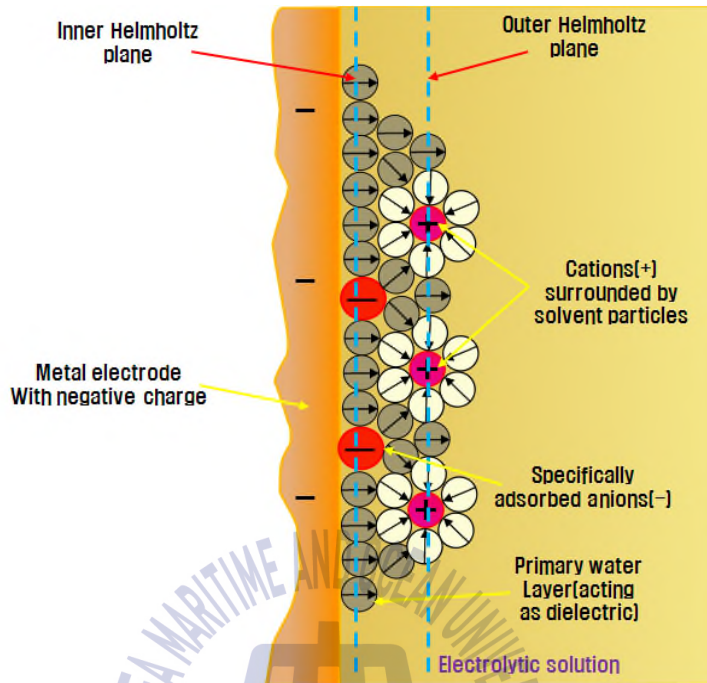


Fig. 2.2 Schematic diagram of electric double layer[27]

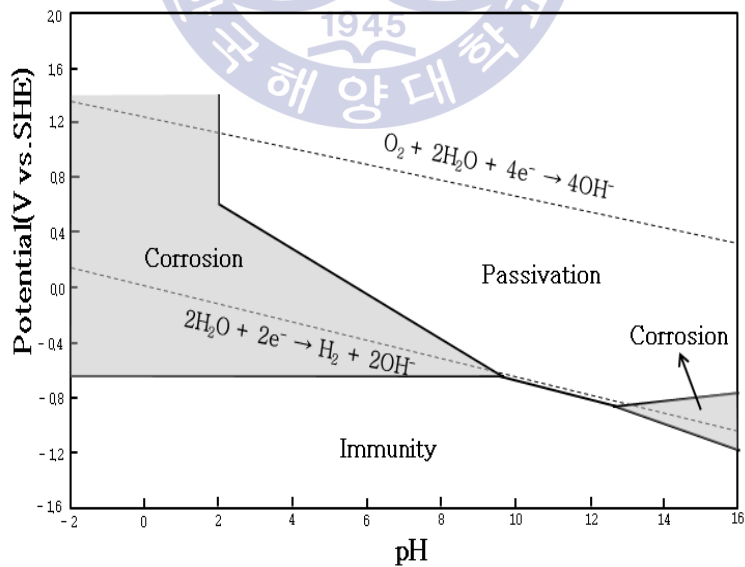


Figure 2.3 Pourbaix diagram for the iron[27]

Table 2.1 Potential value for common secondary reference electrodes [27]

Name	Half-Cell Reaction	Potential V vs. SHE
Mercury–Mercurous Sulfate	$\text{HgSO}_4 + 2\text{e}^- = \text{Hg} + \text{SO}_4^{2-}$	+0.615
Copper–Copper Sulfate	$\text{CuSO}_4 + 2\text{e}^- = \text{Cu} + \text{SO}_4^{2-}$	+0.318
Saturated Calomel	$\text{Hg}_2\text{Cl}_2 + 2\text{e}^- = 2\text{Hg} + 2\text{Cl}^-$	+0.241
Silver–Silver Chloride	$\text{AgCl} + \text{e}^- = \text{Ag} + \text{Cl}^-$	+0.222
Standard Hydrogen	$2\text{H}^+ + 2\text{e}^- = \text{H}_2$	+0.000



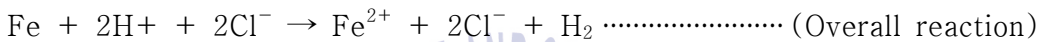
2.1.3 Electrochemical reactions in aqueous

Iron in hydrochloric acid is shown electrochemical reaction as follows:



Pure iron is changed by hydrochloric acid to ferrous ion due to providing electrons with hydrogen ion. Moreover, two ions liberated are absorbed by hydrogen ions and hydrogen ion will be hydrogen gas spontaneously on iron surface.

Next, ionic form reaction is



Overall reaction is separated as follows:



Ferrous ion reaction, defined as the anodic reaction, is an oxidation as iron valence increases from 0 to +2. On the other hand, hydrogen gas reaction, defined as the cathodic reaction, is an reduction where the oxidation of hydrogen decreases from +1 to 0 because of using electrons. The above overall reaction is shown schematically in Figure 2.4.

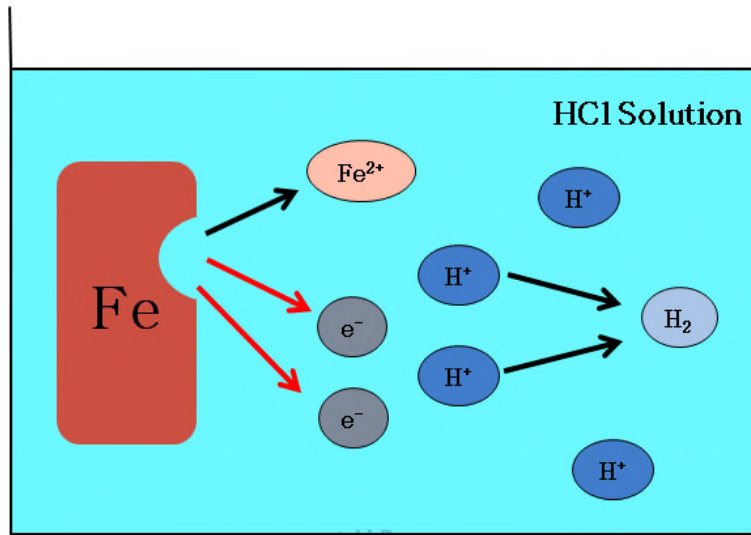


Figure 2.4 Electrochemical reaction in HCl solution



2.1.4 Polarization

Polarization is called the potential deviation of metal surface from equilibrium potential in electrochemical reaction. For instance, iron is in hydrochloric acid. Iron atoms are dissolved continuously to ferrous ions in liquid phase and then the interface of iron becomes more positive by liberating electrons. that is, this positive potential change is called anodic polarization. In the other, the interface of solution will be negative potential change accumulated by electrons which is called cathodic polarization.

The polarization represents as follows:

$$\eta_{total} = \eta_{act} + \eta_{con} + IR$$

η_{act} : activation polarization

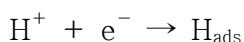
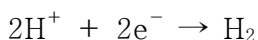
η_{con} : concentration polarization

IR : voltage drop

1) Activation polarization

If the rate of current stream is controlled by some steps on half cell reaction, this is activation, electrons movement or activation polarization.

For example, there are important three steps about hydrogen reaction at metal surface.



First, absorbed hydrogen atom is created by reacting hydrogen ion(H⁺)

and electron from metal at surface. Next, two absorbed hydrogen atoms form hydrogen molecule. Finally, if sufficient hydrogen molecules are on metallic surface, they combine with each other to form hydrogen gas. In reaction, some steps can control the reaction rate and result in activation polarization.

the equation related to activation polarization and current density is as follows :

$$\eta_a = \beta_a \log \frac{i_a}{i_o}$$

$$\eta_c = \beta_c \log \frac{i_c}{i_o}$$

η_a : Anodic polarization

η_c : Cathodic polarization

β_a : Tafel constant on anodic reaction

β_c : Tafel constant on cathodic reaction

i_a : Anodic current density

i_c : Cathodic current density

i_o : Exchange current density

For anodic polarization through above equation, η_a and β_a are positive because the electron on metal surface is removed. On the other hand, for cathodic polarization, η_c and β_c are negative due to collecting the electrons. In addition, β_a and β_c are Tafel constant and then are affected by polarization. Therefore, the relation of polarization and current density shows the numerical value of reaction rate. Tafel behavior of hydrogen

activation polarization is shown in figure 2.5.

The position with $\eta_a = \eta_c = 0$ represents $i_o = i_a = i_c$ on the graph. Moreover, $i_{o,H_2/H^+}$ is called exchange current density. For same value of anodic current density and cathodic current density, that is, rate of oxidation reaction and reduction reaction equals. net reaction doesn't occur.

2) Concentration Polarization

Cathodic reduction reaction decreases at high rate because ions between the electrolyte surface and the adjacent solution relatively were dwindled. That is, the concentration polarization occurs electrochemical reactions by diffusing ions in liquid. So, the concentration is a major key on cathodic reduction reaction.

the equation about the concentration polarization is

$$\eta_{con} = \frac{2.3RT}{nF} \log \left[1 - \frac{i_c}{i_L} \right]$$

the concentration polarization (η_{con}) suddenly is low if it approach a limiting current density (i_L). The limit current density is most high reaction rate but can't be exceeded as a limited diffusion rate in solution.

The equation of limited current density is as follows ;

$$i_L = \frac{D_z n F C_B}{\delta}$$

n : the number of equivalents exchanged

F : Faraday's constant (96,500 coulomb/equiv.)

D_z : the diffusivity of the reacting species

C_B : Concentration of ions in solution

δ : thickness of Nernst's diffusion boundary layer

3) Polarization resistance

Polarization resistance is potential change to be lower by resistance of oxidized film on electrolyte surfaces or by that of solution.

IR drop by solution generally arises from the environment that it is the resistance polarization.

The resistance of solution is represented by Ohmic's law as follows ;

$$R = \frac{l}{kS}$$

R : resistance of solution

l : length

k : electrical conductivity

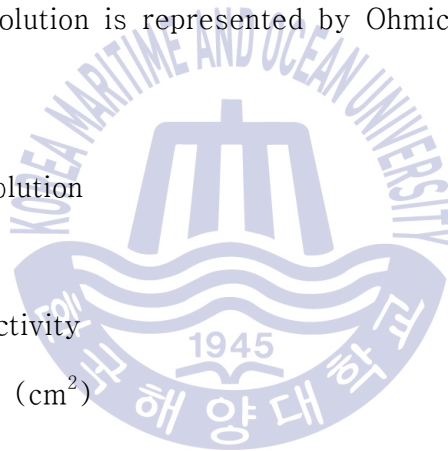
S : area of solution (cm^2)

IR Drop in the solution is

$$IR_{Drop} = I \times \frac{l}{kS}$$

$\frac{I}{S}$ is the current density(i) at IR-Drop. IR-Drop is calculated as follows ;

$$IR_{Drop} = \frac{il}{k}$$



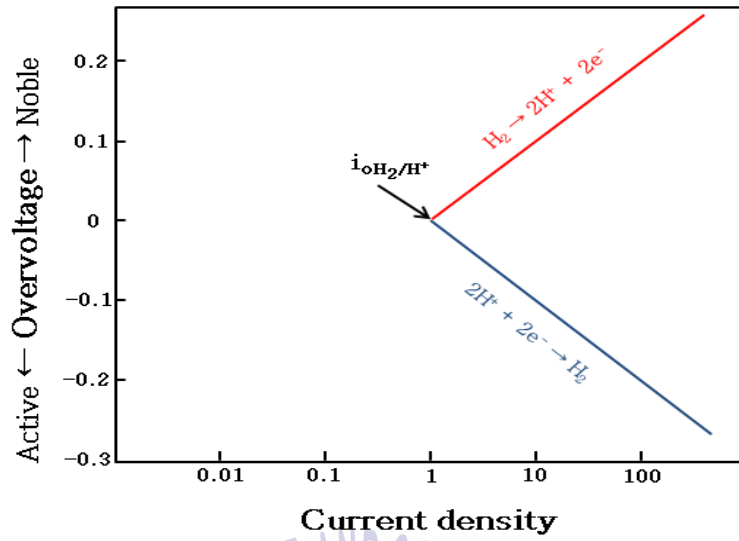


Figure 2.5 Activation overvoltage tends to Tafel's region [27]



2.1.5 Passivity

Very thin oxidized film, called passivity, is formed when a certain metals and alloys are in corrosive solution. Thus, the metal would be able to be protected against the corrosion.

1) Passive films

The passivity is defined a example of corrosion resistance because it is formed thin film in oxidized and high anodic polarization environments. This oxidized film allows metals and alloys to slow the corrosion rate in activation potential circumstance and anodic polarization.

The process of forming passive film is as follows ;



There is a shortcoming of passive film which is brittle. If it was broken by physical and chemical effects, leading to severe corrosion on the metal.

2) Activity and Passivity behavior

It is found prominent difference at area of activity, passivity or transpassivity if metals and alloys are in deaerated acid solution with doing anodic polarization as shown in Figure 2.6. Anodic current density increases with potential value to Passive Current(i_{crit}). At that time, potential value is passive potential(E_{pp}). After that, the oxidized film is formed and then the anodic current density is decreased. Besides, it maintains at a constant current density and the potential is increased continuously at passivity area. However, as the potential is increased constantly, the passive film is broken after approaching to the threshold.

In addition, the anodic current density is increased sharply. Finally, it enters to the transpassivity area and occurs the corrosion again.



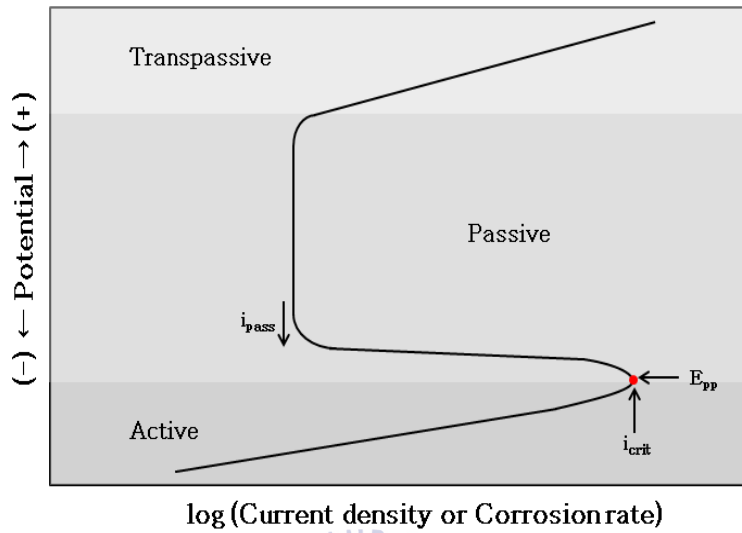
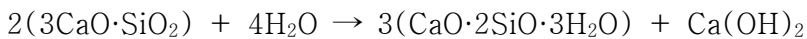
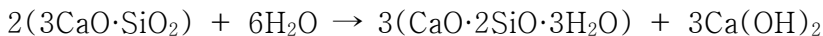


Figure 2.6 Schematic polarization behavior



2.2 Corrosion of steel in reinforced concrete

Concrete generally have been used for a construction material. The concrete mainly is composed with CaO, SiO₂, and Al₂O₃, etc. If these factors are faced with water, the chemical reaction called hydration reaction occurs quickly. Next, the hydration reaction between concrete and water shows as follows ;



Calcium hydroxide (Ca(OH)₂) is found that it had generated such as the above chemical formula. The calcium hydroxide formed by chemical reaction makes neutral environment to high alkaline about pH 12~14. In addition, the concrete has a strong point which is high compressive strength. But tensile strength of this is weak. Thus, the reinforced concrete embedded rebars is invented to be able to overcome the shortcoming of concrete because the concrete and the rebar complement each other. That is, the rebar enhances the tensile strength of concrete. Initially, the surface of rebar in the concrete is formed the passive film in the high alkaline environment. Additionally, the corrosion rate is decreased due to the passivity of rebar surface. This details are shown in Figure 2.7.

In case of changing the alkaline environment to the neutral or being broken the passivity, however, the steel in the concrete is corroded severely. This is because corrosion-affected RC structures are more prone to cracking than other forms of structural deterioration.[6] For processing the steel corrosion, the volume of steel is increased and the concrete is broken easily. Moreover, when the steel is exposed in corrosive environment, the rate of corrosion goes up sharply.

Consequently, the corrosion inducing with cracks destroys the integrity of the concrete cover because it deteriorates the bonding strength of the interface between reinforcement and concrete. And it leads to premature failure of RC structures.[6]



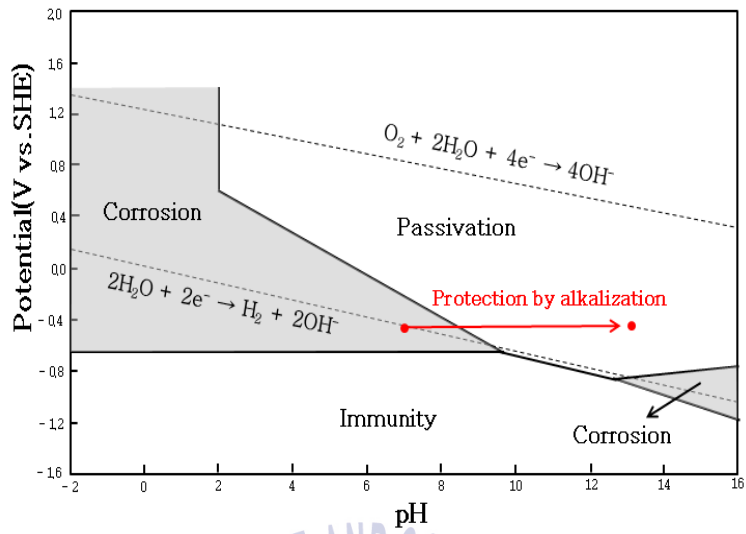


Figure 2.7 Pourbaix diagram for the iron in the concrete



2.3 Corrosion of steel by chloride in reinforced concrete

Steel in concrete generally is stable because steel surface is formed oxidize layer in pH 12~14 environment. By changing the variable factors, however, corrosion of steel in reinforced concrete begins. One of them is pH change by carbonation which leads to the reaction between carbon dioxide(CO_2) and concrete hydrates ; Calcite CaCO_3 and water is produced.

Chloride is the most important factor to corrode steel in concrete. Many studies have been examined about chloride attack.

When Cl^- reaches the reinforcement surface and under normal conditions(presence of oxygen and water), corrosion can be triggered[13]. Exceeding a certain Cl^- concentration threshold, and from a determined electrochemical potential of the steel (mainly related to the O_2 presence in its surface), its protective oxide film (passive layer) starts to be affected by pitting corrosion[13]. As described earlier, the pitting corrosion primarily is caused by chloride ions. the process of this corrosion is different from that of general corrosion as shown in Figure 2.8.

In concrete environment, passive layer on the steel surface is formed in concrete circumstance but it is very thin and easy to be broken. thus, chloride ions induce pitting corrosion because these break down the certain parts of passive layer of steel in concrete and make steel atoms dissolve to ferrous/ferric ions. that is, hydrochloride acid produced by the chemical reaction between hydrogen ion and chloride ions rapidly accelerated the rate of corrosion. Figure 2.9 is pH–potential diagram representing steel corrosion in chloride environment.

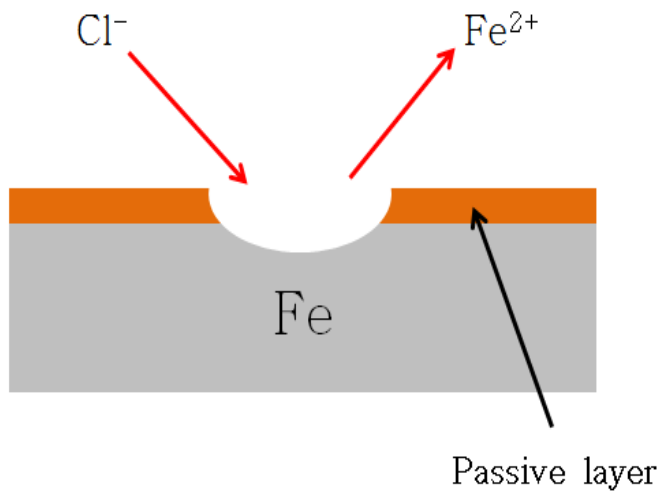


Figure 2.8 Pitting corrosion after being broken passive layer by the chloride content

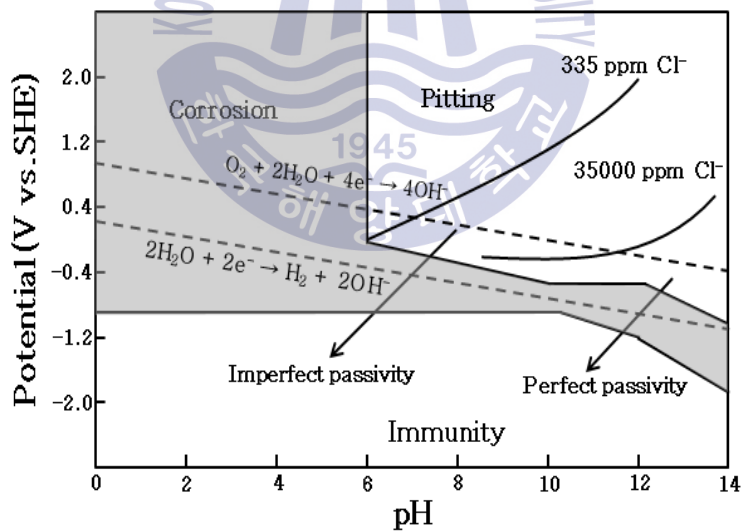


Figure 2.9 E-pH diagram for the iron in chloride environment[28]

2.4 Cathodic protection of reinforced concrete

Cathodic protection is applied widely as a method of protecting against the corrosion. The principal of cathodic protection is explained simply as follows. To begin with, an external anode is needed to flow protection current to the cathode(rebar). the protection current makes the potential of rebar to go down to the immunity area on the pourbaix graph. Therefore, the rebar was protected from the corrosion by CP. Additionally, the cathodic protection can be achieved in two ways; by sacrificial anode cathodic protection or by impressed current cathodic protection (ICCP)[2, 18–19]. That is, those is separated by the way of supplying the protect current and the detail of cathodic protection is shown in chapter 2.4.1 and 2.4.2.

2.4.1 Sacrificial Anode Cathodic Protection(SACP)

SACP is cathodic protection method which is composed of connecting noble and active metal as shown in Figure 2.10. Thus, galvanic current generates by metals having different potential, which protects the noble metal and dissolves the active metal spontaneously. And then electrons flow from the noble to the active. SACP also is known as galvanic protection.

The sacrificial anode commonly is used such as magnesium(Mg), zinc(Zn) and aluminum(Al)[22–23]. A simplified polarization diagram for the SACP is shown on Figure 2.11.

First, the steel is at the point C before connecting the sacrificial anode. At the point C, the corrosion potential and current density is respectively $E_{\text{corr,Fe}}$ and $I_{\text{corr,Fe}}$. Thus, in this anodic polarization, the potential and current density of steel are increased more than those at initial point B.

That is, the corrosion of steel occurs continuously. However, the position of steel is changed by the protection current to the position B after connecting the zinc anode. At the position B, the potential and current density are decreased more than those at the point C. The position of zinc anode(sacrificial anode) is changed from the point E to D by the anodic polarization. Although the zinc anode is corroded, the steel is protected the corrosion by the protection current because it flows from the anode(Zn) to the cathode(Fe). Conclusively, the steel is depolarized to the point B and protected by the protection current from the sacrificial anode.



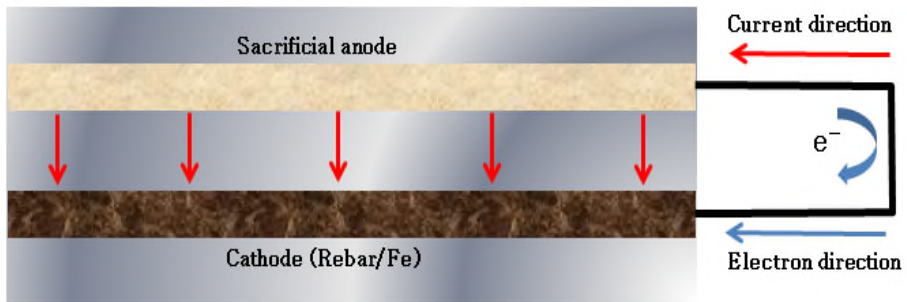


Figure 2.10 The sacrificial anode cathodic protection system

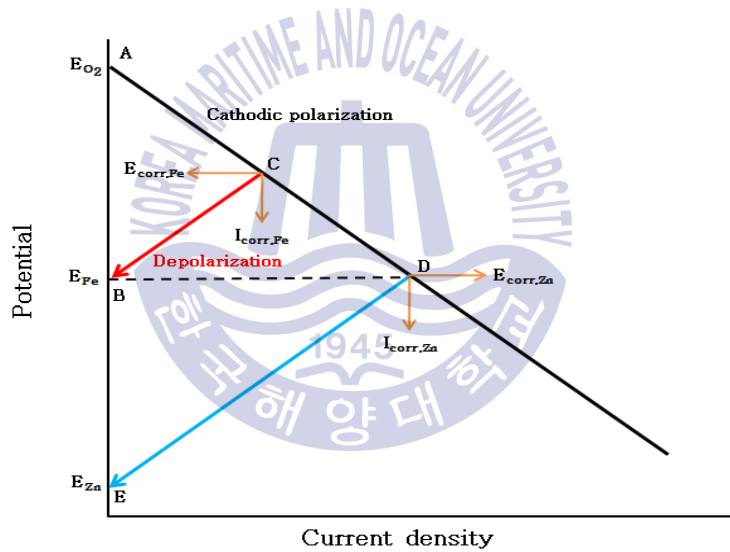


Figure 2.11 Typical polarization curve in SACP

2.4.2 Impressed Current Cathodic Protection system (ICCP system)

Impressed current cathodic protection is a cathodic protection system which constantly supplies impressed current from anode to cathode as shown in Figure 2.12. That is, electrons flow from the anode to the cathode (metal needed corrosion protection). The anode such as platinum (Pt), titanium (Ti), lead (Pb) and niobium (Nb) is utilized in the ICCP system because it is insoluble and high resistance. A simplified polarization of ICCP is shown by the Figure 2.13.

Oxygen (O_2) reduction reaction occurs with cathodic polarization from position A to C. In addition, oxidation reaction occurs on the steel surface with anodic polarization from point B to C. At point C, potential of the steel is corrosion potential (E_{corr}) and current density of the steel is corrosion current density (I_{corr}); the dissolution of steel is begun.

However, by using the power supply, anodic polarization is changed from position C via B' to point B on the line and the potential and current density are decreased gradually. On the other hand, the reduction reaction in the oxygen is increased from point C via point C' to point D. When the insufficient current is supplied on the system, the steel is protected partially with the potential of position C to B' and current density of $i_{C'} - i_B = \Delta i'$. Therefore, If sufficient current is supplied for the system, the steel is completely protected with the potential of position B to D and current density of $i_{C'} - i_B = \Delta i$.

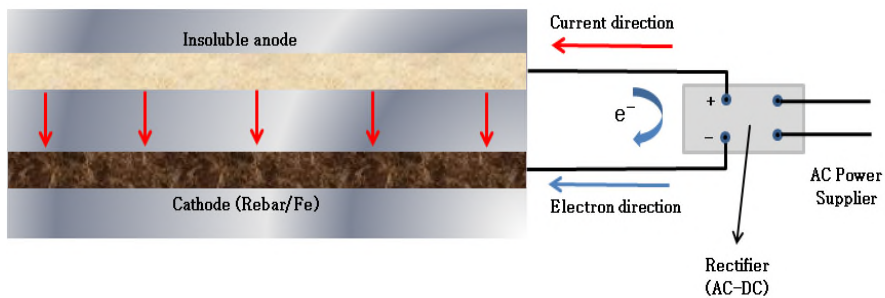


Figure 2.12 Impressed Current Cathodic Protection system

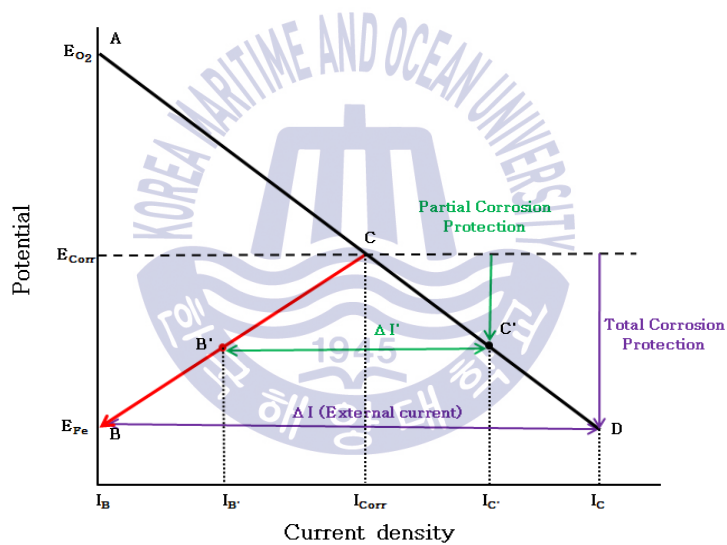


Figure 2.13 Typical polarization in ICCP

Chapter 3

LITERATURE REVIEW

3.1 Availability of cathodic protection in reinforced concrete

Cathodic protection is a way to change the position from corrosion area to immune area by using electrons. Besides, cathodic protection is divided two methods which are sacrificial anode cathodic protection(SACP) and impressed current cathodic protection(ICCPC). These ways respectively have merits in order to be installed on the structures and other systems. So, a number of authors have studied the cathodic protection to prohibit the corrosion of metals. Although the purpose of their study is respectively different, most of studies is both the feasibility and the cathodic protection efficiency.

C. Christodoulou et al. [1] evaluated the long period benefit of ICCP. They tried to search the merits of ICCP system through a number of test on the structures. thus, the existence of persistent protective effects was found that it had occurred by ICCP. Figure 3.1 shows the corrosion rate from the polarization resistance test. In Figure 3.1, passive layer is maintained for 24 months at least after using ICCP for 5 years and more.

Guofu Qiao et al.[4] studied the numerical optimization method of ICCP system for RC structures. The numerical model of the ICCP is built to find the optimal cathodic protection way. After conducting the experimental test, they compared with the simulation. the result of numerical optimization and experimental about the potential of the steel is shown by

Table 3.1.

Xun Xi et al.[6] studied the time to occur surface crack and crack width on the structure by the corrosion. they tried to find the time to be surface crack by the corrosion and mechanical parameters on the simulation. By the simulated models, they found that the factors which are breaking the structures like ambient temperature, chloride content and corrosion rate affected on the time. The Figure 3.2 shows the results related to the corrosion, cracking and time. when the steel constantly is corroding , the volume of this gradually is increasing. thus, the concrete is broken and the corrosion rate sharply is increasing.

Keir Wilson et al.[12] investigated the selection and use of cathodic protection systems for the repair of reinforced concrete structures. they had compared the benefits, practicality, economic feasibility of CP between ICCP and SACP. The factors comparing on the research are the service life, constructing cost and repairing cost, etc. They found the results through their experience that SACP is proper to small and target repair. In addition, It is suitable to apply it on the structures whose service life is less than 10 years. Reversely, ICCP is a significant way to protect the corrosion of steel in concrete. This system can be utilized large structure in which service life is more 25 years and great area in corrosion environment.

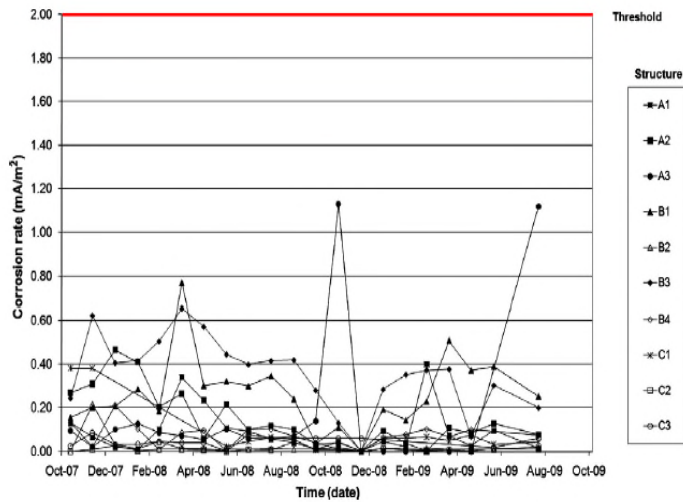


Figure 3.1 Corrosion rates summary from polarization resistance test[1]

Table 3.1 Results of test for the potential of the reinforcing steels [4]

Steel bars No.	Measured points No.	Optimization results (V vs. SCE)	Experimental results (V vs. SCE)		Relative errors	
			T-shaped beam #1	T-shaped beam #2	T-shaped beam 1#	T-shaped beam #2
I	1	-0.766146018	-0.747	-0.784	-2.56%	2.39%
	2	-0.767684295	-0.768	-0.790	0.04%	2.91%
	3	-0.76614686	-0.755	-0.804	-1.48%	5.01%
II	4	-0.766154377	-0.791	-0.756	3.14%	-1.28%
	5	-0.767686269	-0.788	-0.788	2.58%	2.58%
	6	-0.766133304	-0.749	-0.766	-2.29%	-0.02%
III	7	-0.817092219	-0.835	-0.775	2.14%	-5.04%
	8	-0.826175849	-0.909	-0.817	9.11%	-1.01%
	9	-0.816840867	-0.875	-0.893	6.65%	8.70%
IV	10	-0.750325697	-0.773	-0.761	2.93%	1.38%
	11	-0.766622388	-0.798	-0.796	3.93%	3.68%
	12	-0.750123242	-0.760	-0.811	1.30%	8.01%
V	13	-0.750083001	-0.789	-0.799	4.93%	6.20%
	14	-0.766379668	-0.804	-0.829	4.68%	7.79%
	15	-0.750186879	-0.752	-0.805	0.24%	7.29%
VI	16	-0.816836173	-0.873	-0.780	6.43%	-4.22%
	17	-0.826463067	-0.973	-0.870	15.06%	4.47%
	18	-0.816511493	-0.845	-0.840	3.37%	2.78%

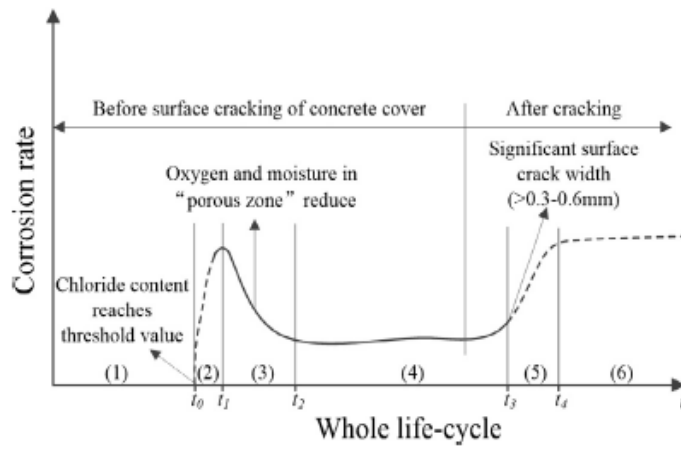
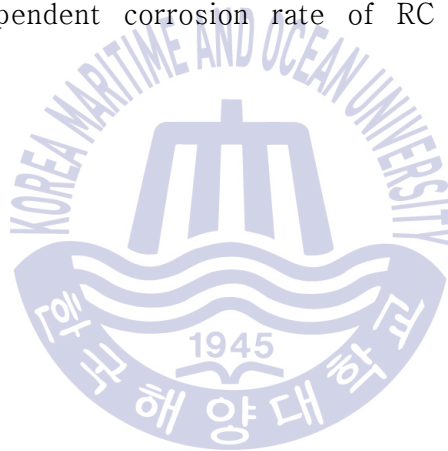


Figure 3.2 Time-dependent corrosion rate of RC structures during the whole life-cycle[6]



3.2 Effect of CP in chloride environment

Chloride contents commonly is a major factor to occur the corrosion of metals on the structures. The major problem such as spalling and cracking on the concrete generally occurs because the chloride ions continuously invade to the concrete in seawater. In addition, they allow the environment in the concrete to change and induce the corrosion severely. A plenty of studies are investigated by many authors as the chloride ions make severe problems on the concrete structures.

Binbin Zhou et al[9] examined electrochemical parameters related to corroded rebars in concrete under chloride environments. They studied Polarization behavior of activated reinforcing steel bars (rebars) in concrete by using of measured cathodic polarization curves. Moreover, the polarizaion behavior of rebars in concrete is evaluated by five factors which are relative humidity, Cl^- content, rebar diameter, water-cement ratio and corrosion duration. They found that Cathodic exchange current density has the most significant effects on corrosion rate and A practical model for the corrosion rate of rebars in concrete is proposed.

J. Carmona Calero et al.[13] studied how different ways of chloride contamination can affect the efficiency of cathodic protection. In this studies, they utilize two different versions of cathodic protection on lab specimens. And then two different ways were applied permanent immersion in a NaCl solution and periodic pouring of discrete amounts of a NaCl solution with atmospheric exposure. they found the useful results which are particular features on the study in each case.

The measurements of depolarization of each one of the electrochemically

treated samples 7 days after the switch off are seen at Table 3.2.

Luca Bertolini et al.[17] investigated the throwing power of cathodic prevention with sacrificial anode. They tried to find the throwing power data in partially submerged marine reinforced concrete file. They also compared the experimental test and the simulation programs installed the sacrificial anodes immersed in the seawater is made to investigate throwing power and corrosion condition of the examine. Figure 3.3 indicates the depolarization of the test with cathodic protection and cathodic prevention. The distributions of potential per the depth gained by this test are represented by Figure 3.4.

Luca Bertolini et al.[25] studied the sacrificial anode for cathodic protection in seawater. They conducted the experimental test which is compare the effects of sacrificial anodes on passive steel and corroding steel on reinforced concrete columns. For the steel, it is divided to in chloride free concrete and chloride contaminated concrete. Figure 3.5 represents the potential distribution of the steel with and without chloride during depolarization. Moreover, the submerged zone of reinforced concrete columns was depolarized to 200mV. The results show that the sacrificial anodes are an effective and economic method for preventing corrosion in submersed zone.

Table 3.2 The measurement of polarization after switching off[13]

Routes of contamination	Samples	Cl ⁻ content average (% relative to cement mass)	Cl ⁻ content in rebar vicinity (% relative to cement mass)	Depolarization at 7 days (mV)
A contamination	ACP	5.59	3.92	217
	ACPre	5.48	3.23	211
B contamination	BCP	5.38	3.07	487
	BCPre	3.94	2.61	153

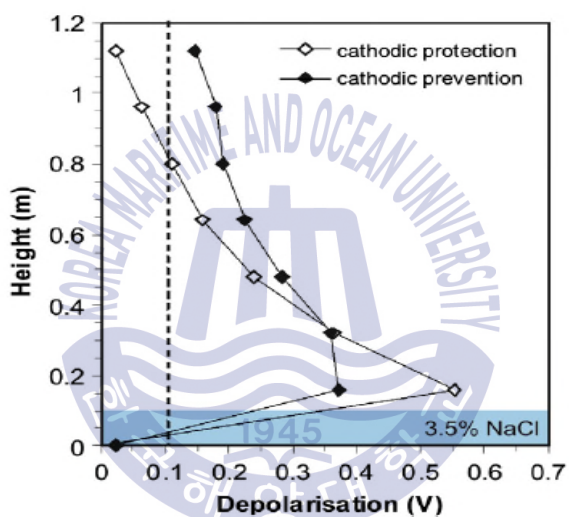


Figure 3.3 The depolarization test compared the cathodic protection and cathodic prevention[17]

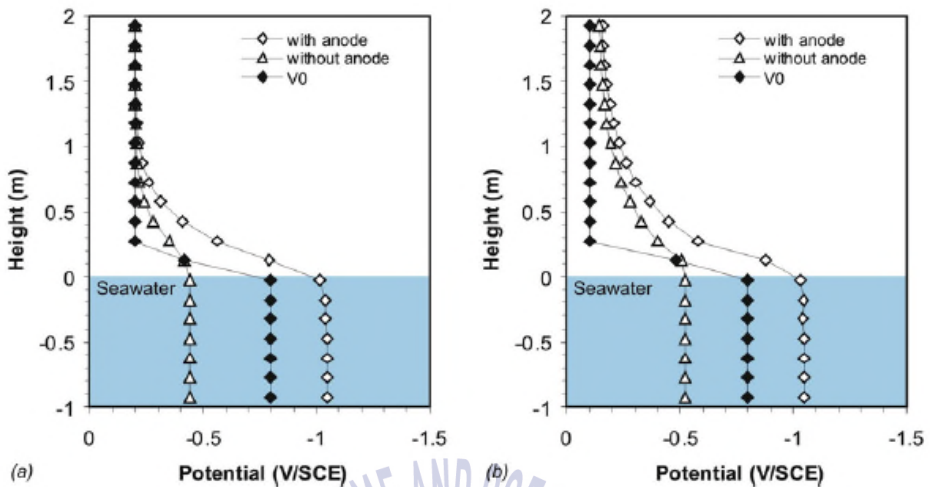


Figure 3.4 Comparison between throwing power of potential obtained from the numerical models[17]

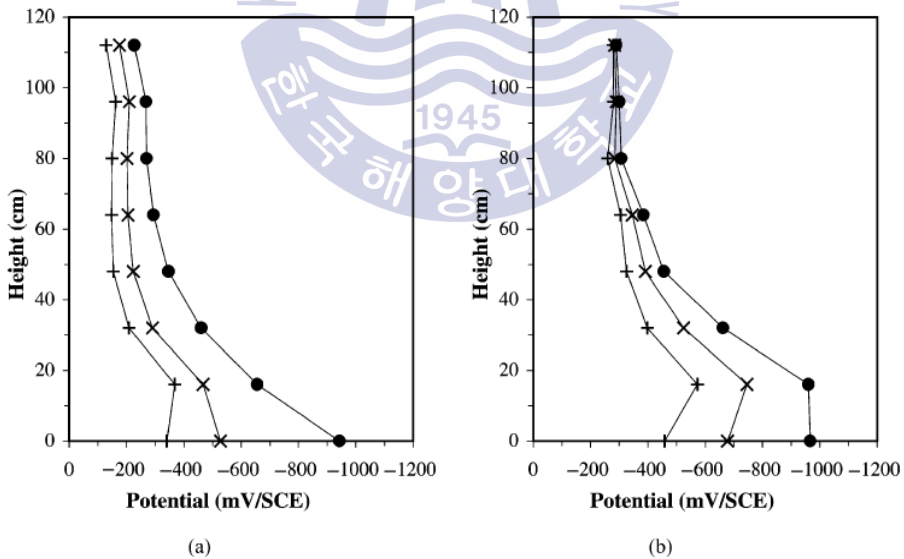


Figure 3.5 Potential distribution of steel in concrete (a) without chlorides and (b) with 3% chloride by weight of cement during a depolarization test carried out after 24 months of CP application[25]

3.3 Arrangement and type of anode for ICCP in RC

As mentioned earlier, the ICCP system generally is considered a attractive way to protect corrosion of various metals and alloys. And this method globally has been used to extend the service life of structures. a number of studies about using ICCP in the reinforced concrete is examined by many authors. These studies are focused that how effect the kind and arrangement of anode for ICCP are.

Prasad V. Bahekar et al.[2] investigated in the effectiveness of ICCP used the anode as CFRP laminate. And then they evaluated this by half-cell potential, LPR, bond stress and mass loss at Table 3.3 and 3.4. In addition, the corrosion level is separated by them to three steps. Standard Code of practices have suggested cathodic protection current densities ranging between 2 mA/m^2 and 20 mA/m^2 . However, This study shows that the specimen applied with 5 mA/m^2 in all the three corrosion levels exhibited lowest ratio. Thus, this study concludes that the most appropriate protection current density against corrosion in all corrosion levels is 5 mA/m^2 because it ensures longer service life of RC structures that are vulnerable to rebar corrosion.

Mochammad Syaiful Anwar et al.[3] studied Lightweight cementitious anode for ICCP system using pumice aggregate (PA). The anode is composed as follows ; pumice aggregate (fine), carbon fibres and cement with MMO-Ti. The examination is conducted the process such as accelerated galvanic test, conductivity measurement, dry density and compressive strength. In addition, It compared with the cement mortar without fibres. In conclude, the weight loss of the anode occurred and

reduced the half of the weight. They assert these anodes is proper to use as an anode for cathodic protection verified by polarization and impedance test. Figure 3.6 represents the polarization curve of 50% pumice mortar containing 0.7% CF that it is stable passive area from the potential value of 600 – 2500 mV.

Ji-hua Zhu et al.[7] studied the corrosion protection using ICCP and structure strengthening technique for the columns. The potential values of the rebars on all the specimens are shown in Figure 3.7. The compression capacity and deformation of the column are recorded at Table 3.5. They argued the ICCP–SS system is not only effective to protect the corrosion of the steel but also improves durability against the compression force of the corroded columns.

Jing Xu et al.[15] studied the current distribution of impressed current protection with conductive mortar overlay anode in reinforced concrete. The results of initial half cell potential and corrosion rate with or without chloride is indicated by Table 3.6. Table 3.7 shows another important effect of concrete resistivity on the current distribution is discrepancy among the currents by the rebars present at different cover depths. The ratio of average value of current within each layer of rebar is shown in Table 3.8.

The results measured this test represent the initial corrosion rate on the steel has effect on the protection current distribution. Moreover, the corrosion rate has limited value.

Table 3.3 Corrosion rates at the low corrosion level[2]

Exposure (Days)	Corrosion rate, I_{corr} (mA/m ²)				
	L C	L 2	L 5	L 10	L 20
0	29	13	-	16.9	21.7
15	42.1	13.3	11.3	11.8	15.7
30	41.8	10.4	7.71	9.3	16.7
45	55.5	10.9	6.78	8.74	17.6
60	43	8.81	5.55	6.93	10.4
	M C	M 2	M 5	M 10	M 20
0	61.7	0.291	26.1	50.2	46
15	80.6	22.9	23.9	49.9	41.1
30	81.6	21.2	23.4	41.9	38.7
45	96.5	20.1	21.4	45.3	25.9
60	119	18.8	17.7	38.3	33.2
	H C	H 2	H 5	H 10	H 20
0	59	40	59.2	69.2	60.6
15	77.7	56.7	56.6	84.6	54.3
30	88.8	49.3	55.1	77	48.7
45	90.9	52.1	53.5	59.9	37.9
60	95.1	55	48.4	49	33.1

Table 3.4 Bond stress, slip and % mass loss at the whole corrosion level

Specimen	Bond Stress (N/mm ²)	Slip (mm)	% Mass Loss	% Mass loss/Bond Stress
L C	11.74	13.65	6.53	0.56
L 2	10.75	13.84	6.41	0.60
L 5	11.38	13.12	6.35	0.56
L 10	10.37	12.67	6.22	0.60
L 20	9.51	11.70	6.05	0.64
M C	8.48	11.84	13.60	1.60
M 2	8.25	11.40	13.13	1.59
M 5	7.53	11.10	11.80	1.57
M 10	6.67	10.42	12.58	1.89
M 20	6.44	8.97	12.43	1.93
H C	6.13	10.78	20.00	3.26
H 2	5.93	9.86	19.51	3.29
H 5	5.55	8.24	18.12	3.26
H 10	4.24	6.76	18.71	4.41
H 20	1.86	5.23	18.11	9.74

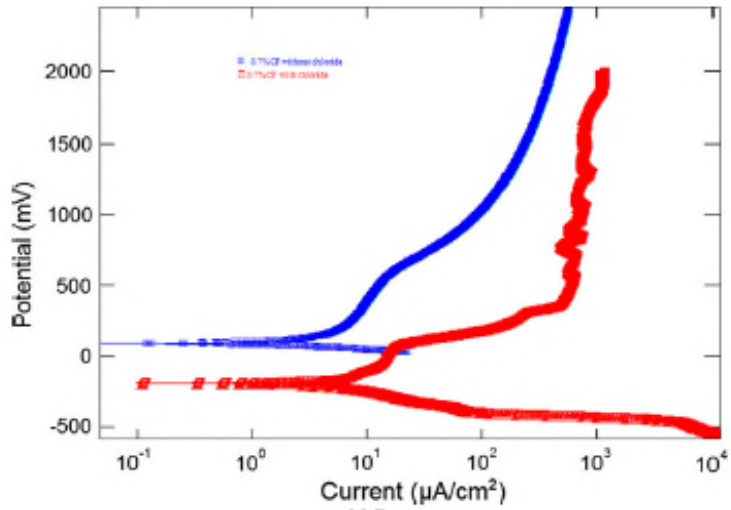


Figure 3.6 The polarization curve of 50% pumice mortar containing 0.7% CF

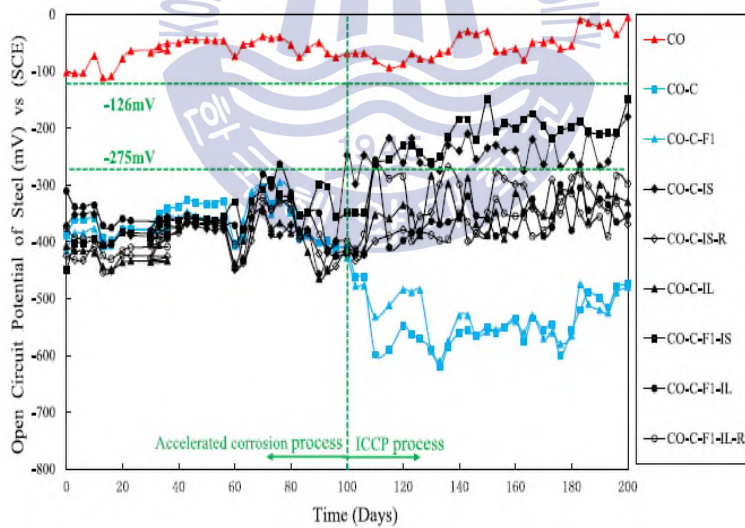


Figure 3.7 The potential of all specimens during the test[7]

Table 3.5 The compression capacity and deformation of the column[7]

Columns	Ultimate load (kN)	Ultimate deformation (mm)	Hoop strain of carbon fiber mesh measured at ultimate loads	Increase in strength compared to control column (CO) (load = 1545 kN) (%)	Increase in strength compared to corroded columns (CO-C and CO-C-R) (average load = 1309 kN) (%)
CO	1545	1.1	-	-	18.0
CO-C	1286	1.9	-	-16.8	-
CO-C-R	1331	1.9	-	-13.0	-
CO-C-FI	1687	2.5	0.0027 [*]	9.2	28.9
CO-C-IS	1605	2.0	-	3.9	22.6
CO-C-IS-R	1520	1.7	-	-1.6	16.1
CO-C-IL	1597	1.7	-	3.4	22.0
CO-C-FI-IS	1801	3.7	0.0018 [*]	16.6	37.6
CO-C-FI-IL	1969	2.7	0.0134	27.4	50.4
CO-C-FI-IL-R	1664	2.0	0.0051	7.7	27.0

Table 3.6 Measurement results of initial half cell potential and corrosion rate[15]

Specimen No.	$E_{\text{corr, SCE}}$ (mV)	i_{corr} (mA/m ²)
1	-581.1	3.3
2	-514.9	6.1
3	-601.9	19.5
4	-562.8	20.6

Table 3.7 Ratio of the average value of current within each layer of rebars for specimens with different concrete resistivity[15]

Concrete resistivity	Specimen no.			
	2		4	
	\bar{I}_1^a/\bar{I}_2^a	\bar{I}_1/\bar{I}_3^a	\bar{I}_1/\bar{I}_2	\bar{I}_1/\bar{I}_3
Low	0.45	0.56	0.80	0.79
Intermediate	0.84	1.61	0.62	1.34
High	2.54	3.13	4.32	5.06

Table 3.8 Ratio of the average value of current within each layer of rebars for specimens with different impressed current density[15]

Current density (mA/m ²)	Specimen no.			
	1		3	
	\bar{I}_1/\bar{I}_2	\bar{I}_1/\bar{I}_3	\bar{I}_1/\bar{I}_2	\bar{I}_1/\bar{I}_3
10	1.00	1.69	1.00	1.65
20	1.09	1.79	1.36	2.17
40	1.41	1.61	1.59	2.20

Chapter 4

EXPERIMENTAL PROCEDURES

4.1 Specimens

The specimens are divided two-type according to their pattern such as beam and slab in order to find a optimal impressed current protection system. In method of cathodic protection at present, it uses only one type of anode for protecting against corrosion but there is a problem that it would not be able to supply constant protection current to the specimen perfectly. In this study, the diverse shapes of anode for ICCP were utilized on the complex structure of the building to find the proper cathodic protection. In addition, those anodes were manufactured to be installed easily on the complicated structure. Concrete mixed design is shown in Table 4.1. The Specimens was built in atmosphere for 28 days and then the reinforced steel was a typical carbon steel for the construction on KS D16(ASTM #5).

A beam type specimen is shown in Figure 4.1. It was created with a base on 100 mm x 100 mm x 250 mm according to ASTM G109. Additionally, the length of two reinforced steels was 350 mm. The container on the specimen is for experimental water.

A slab type specimen was fabricated with six reinforced steels being 700 mm long and these were located at interval of 60 mm each. The slab type was height of 70 mm, width of 400 mm and length of 400 mm. Figure 4.2 represents the slab type specimen with a water container.

Table 4.1 Detail contents of the reinforced concrete specimen

Gmax	Slump	Air	W/C	S/A	Unit quantity(kg)			
					Water	Cement	S	GA
9.5mm	10cm	5%	51%	53.3%	210	411	845	752.4
Remark Gmax = Maximum size of coarse aggregate W/C = water-cement ratio S = Fine aggregate GA = Coarse aggregate								

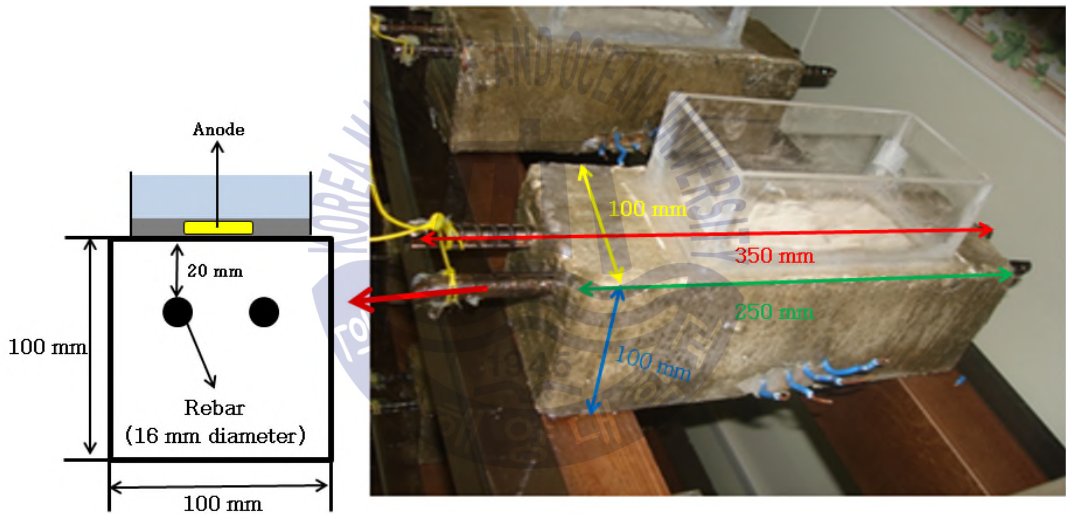


Figure 4.1 Beam type specimen

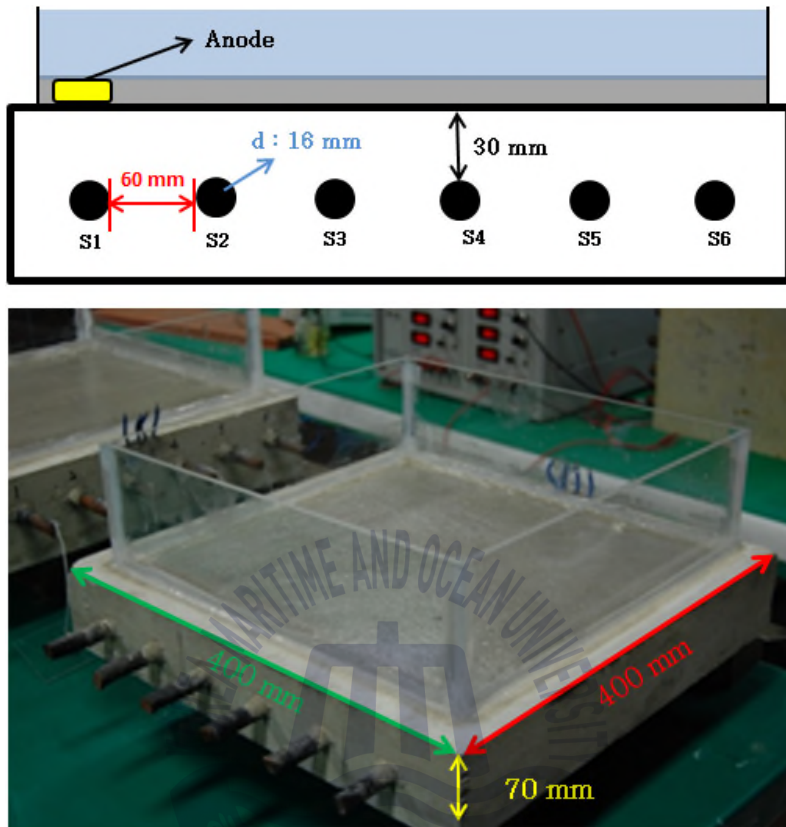


Figure 4.2 Slab type specimen

4.2 Manufacture of anodes for ICCP and installation

Anode for ICCP was separated 3-type in accordance with their shape in order to be installed conveniently. The anode is a insoluble metal such as titanium, which was fabricated to diverse type such as ribbon, rod and mesh.

On the beam type specimens, the anodes such as Ti-Ribbon, Ti-Rod and Ti-Mesh were used for ICCP system. In detail, Ti-Ribbon was 100 mm X 20 mm and Ti-Rod was 90 mm X 10 Φ . Besides, Ti-Mesh was 90 mm X 65 mm. These pictures are seen in Figure 4.3. On the slab type specimen, the anodes of Ti-Ribbon were used with 300 mm X 20 mm and then the Ti-Mesh was 100 mm X 100 mm.

Besides, these anodes respectively were grouted by mortar as shown in Figure 4.4. The anodes were installed on the slab type specimen and then are indicated in Figure 4.5. The anode of Ti-Ribbon was installed parallel on top of first reinforced steel(S1) and the Ti-Mesh was installed top of between the fifth and sixth steel. As shown in Figure 4.5, The Ti-Rod was inserted to the hole which had been drilled 20 mm and this hole was plugged by the mortar.

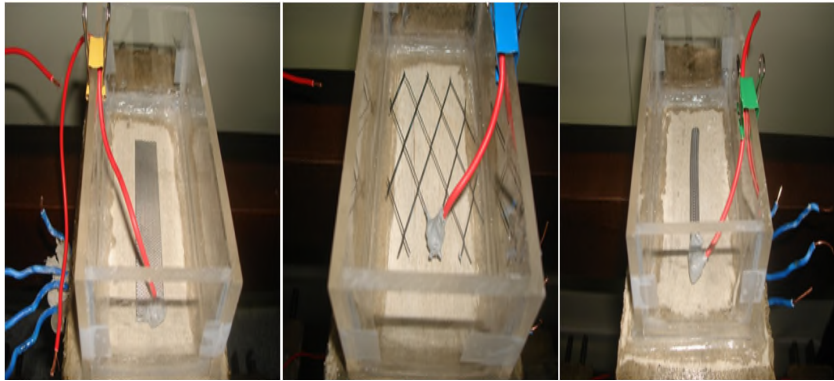


Figure 4.3 Installation of 3 types of anode in the beam type specimens



Figure 4.4 Anode of ribbon and mesh type grouted by mortar

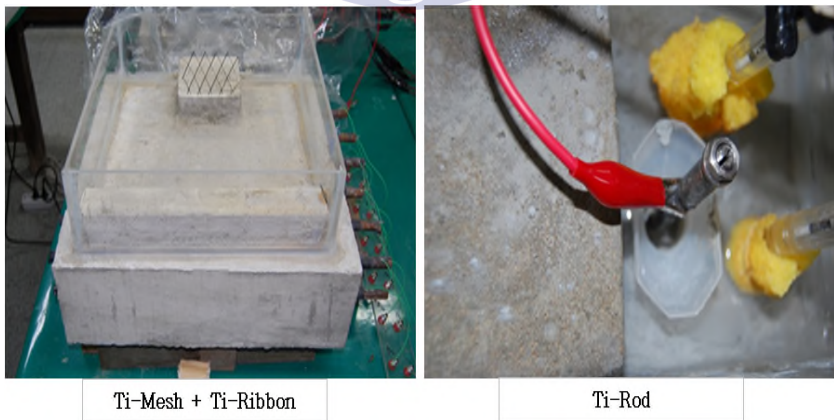


Figure 4.5 Installation of 3 types of anode in slab type specimens

4.3 Installation of test devices

Before installing the test equipments, several processes were conducted in order to carry out the test conveniently. The end of two reinforced steels was made a hole by drill and be connected electric wire to set up the devices for potential measurement and protection on the beam type and slab type specimens. In addition, the wire was fixed by screws. The anodes were located on the end of steel and were fixed by soldering to minimize the contact resistance. Moreover, the contacting part was covered with epoxy and then the current was not to flow. The outside of the specimens except the part of water container was put on the enamel in order to prohibit the evaporation of experimental liquid. Therefore, the liquid was able to be absorbed only through underside.

Figure 4.6 and Figure 4.7 are the picture for cathodic protection on the specimens. The rectifier called CR-1212 Multichannel power supply was utilized to supply CP current, which is able to monitor not only CP potential and current but also 4 hour depolarization potential. As shown in Figure 4.8, the input and output port on the terminal of power supply were connected with the reinforced steel in the specimens, the anodes for ICCP and the reference electrodes to conduct the test. The silver-silver chloride electrode(SSCE) was used as the reference electrode during this study. Six SSCEs were fixed respectively on top of the steel in the specimens as indicated in Figure 4.9. In addition, the porous sponge is applied on the end of the reference electrode to reduce the contact resistance between the concrete surface and it.



Figure 4.6 Picture of cathodic protection test on the beam type concrete specimens

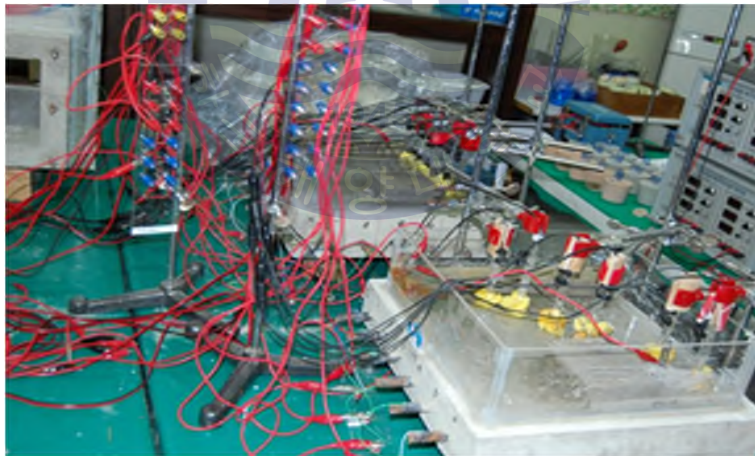


Figure 4.7 Picture of cathodic protection test on the slab type concrete specimens

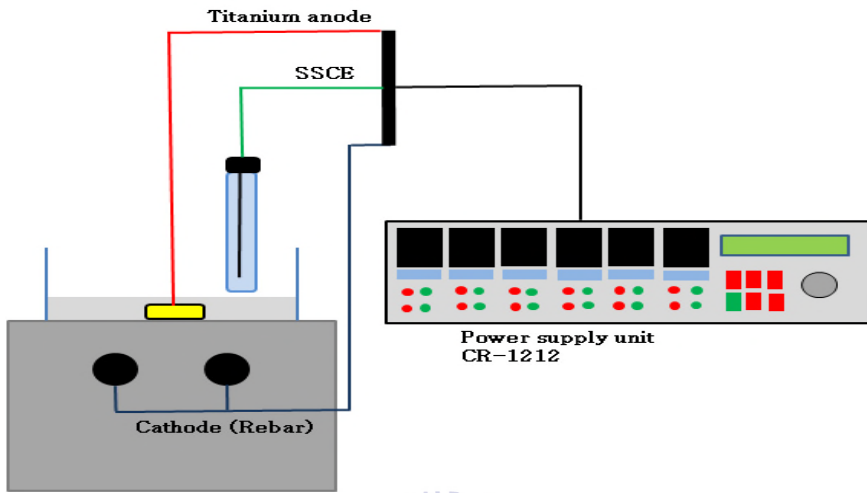


Figure 4.8 Schematic diagram of beam type specimen installed anode and reference electrode for cathodic protection

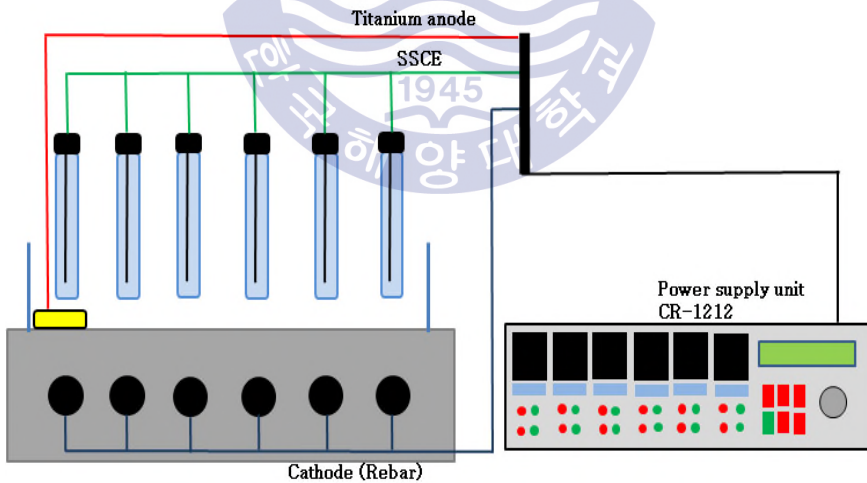


Figure 4.9 Schematic diagram of slab type specimen installed anode and reference electrodes for cathodic protection

4.4 Procedures & analysis

4.4.1 Measurement of E-log i on the specimens

E-log i test is a way which is to confirm the optimum cathodic protection potential on the specimens. Reference 600 potentiostat manufactured by Gamry Instruments co., was conducted the measurement on the specimens as the experimental device as shown in Figure 4.10. On the cathodic polarization curve for the iron, potential values were decreased by the open circuit potential and then current density values were increased during the polarization. However, if these are reached to the constant value, the variation of the current density value will be decreased. In addition, it is found that the position is changed the linear to the de-linear on the graph. This inflection point is called the minimum cathodic protection potential that it implements the cathodic protection. The value of current density at that point is the minimum current density to stop the corrosion.

For this study, E-log i measurement was examined 3 times per each specimens applied ICCP with the titanium anode. The test rate for the cathodic polarization was decided 1 mV/sec by the open circuit potential of the iron from +5mV to -1,000mV. SSCE (Silver-Silver Chloride Electrode) also was utilized as reference electrode for this study.

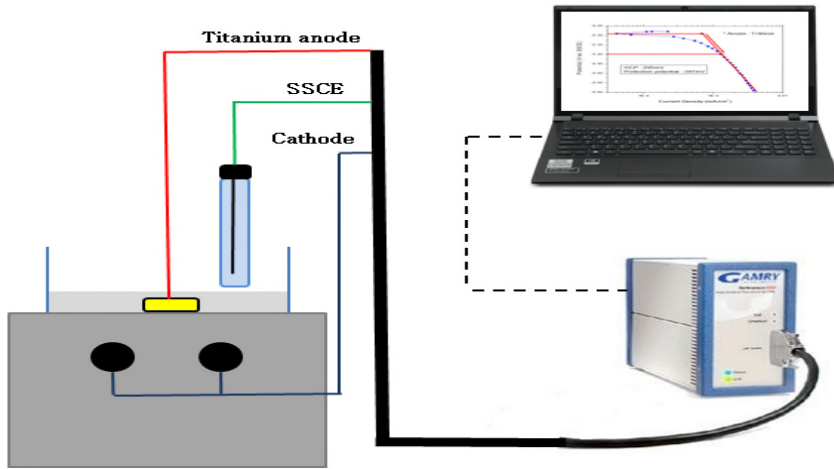
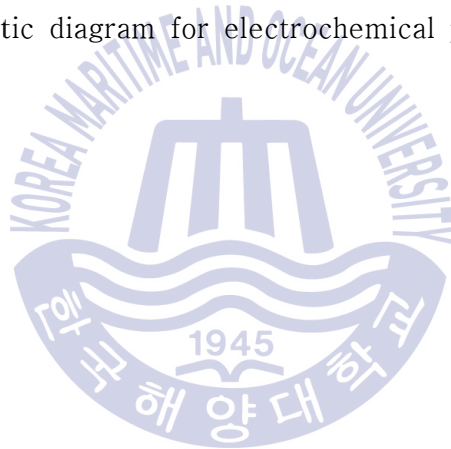


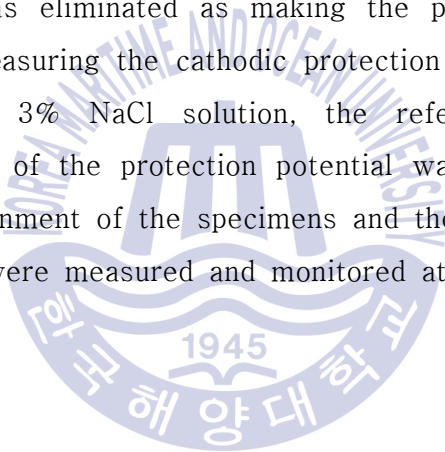
Figure 4.10 Schematic diagram for electrochemical polarization test



4.4.2 Measurement of cathodic protection potential

Silver–silver chloride electrode(SSCE) was used as the reference electrode and then Fluke digital multimeter was applied as the potentiometer during the measurement.

When the specimen of beam type was measured the cathodic protection potential in atmosphere, it is difficult to gauge the value of those because it had the error by contact resistance between the reference electrode and the concrete. So, some sponges with fresh water were attached on the end of reference electrode to remove it. This is because the error by contact resistance was eliminated as making the path of electrolyte. In others case, when measuring the cathodic protection potential of specimen in fresh water and 3% NaCl solution, the reference electrode was submerged. Behaviors of the protection potential was compared according to the exposed environment of the specimens and the anode type. All data values automatically were measured and monitored at interval of 1 minute during the test.



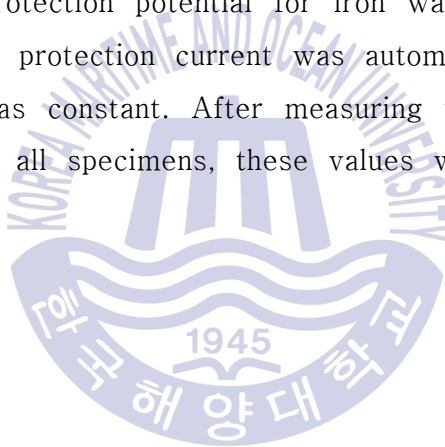
4.4.3 measurement of depolarization potential

The depolarization potential on the specimen was measured to confirm the condition of cathodic protection according to 100 mV depolarization criteria by NACE. When examining the depolarization on the specimen, negative terminal on the supply unit was connected with the rebar of specimen and then positive terminal was linked with the anode of ICCP. Moreover, the protection current was supplied from the anode. In addition, the value of cathodic protection potential was decided by the type of specimens ; it is -900 mV/SSCE in the beam type and -600 mV/SSCE in the slab type. The specimens of beam and slab type also were measured the cathodic protection potential in different corrosive environment such as atmosphere, fresh water and 3% NaCl solution. When powering off on the system temporarily, the potential was rapidly increased. However, the rising rate of potential gradually became slow over time. The initial potential was increased by IR-drop occasionally and then the change of depolarization except the IR-drop was the real degree of depolarization. In this study, 4h decay criteria was adopted. Additionally, in case of slab type specimen, after adding the other anode such as Ti-Ribbon, Ti-Mesh and Ti-Rod at S5 - S6 position, the slab type specimen was measured again.

4.4.4 Measure of cathodic protection current

Cathodic protection current is called the current which flows from insoluble anode for ICCP to the rebar by difference of potential on the power supply. That is, the real protection current is supplied through the vehicle of concrete to the insoluble anode for ICCP. Besides, the cathodic protection current is measured by the electrochemical measurement device having the ZRA(Zero Resistance Ammeter) mode.

Potentiostatic mode on the power supply was adopted to measure the protection current for the specimens in same circumstance. The setting value of corrosion protection potential for iron was -900 mV/SSCE. In addition, the cathodic protection current was automatically controlled and then the potential was constant. After measuring the degree of cathodic protection current on all specimens, these values were compared by the exposed environment.



Chapter 5

RESULTS & DISCUSSION

5.1 Results of measuring E–log i on the beam type specimens

Figure 5.1 shows E–log i graph on the beam type specimen.

The corrosion potential was defined by linearity or Tafel behavior on the graph shown in Figure 5.1. That is, the corrosion potential was -295 mV/SSCE and then the protection potential was -397 mV/SSCE. The difference value was about 100 mV, which met 100 mV depolarization criteria of NACE.

As shown in Figure 5.2, it was difficult to decide the optimal protection potential in accordance with the kind of anode because the prominent tendency was not found. However, when classifying the value of cathodic protection potential on the specimens with all anodes used by the environment, the familiar tendency was found. That is, the numerical value of optimal cathodic protection potential was the highest in atmosphere, followed by the fresh water and sea water. The results indicated that the concrete resistivity on the specimen had major effect on the protection potential. This is because the value of protection potential was increased by that of the concrete resistivity on the specimens in the different environment.

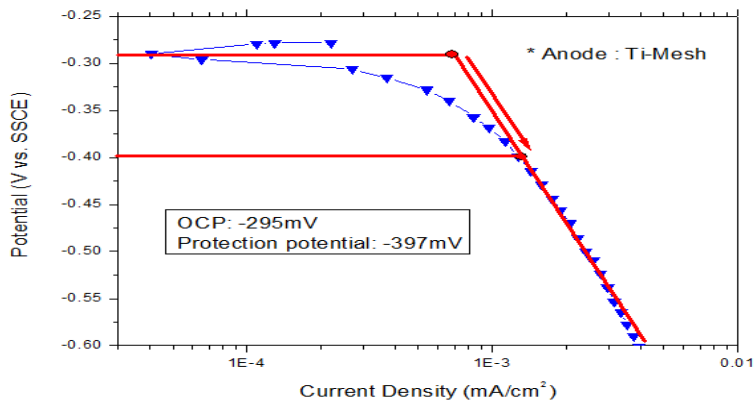


Figure 5.1 E-log i graph for the beam type specimen

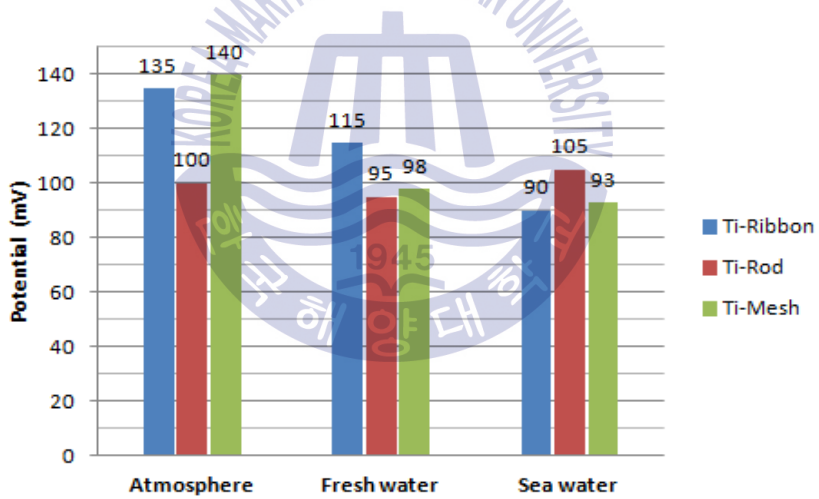


Figure 5.2 Protection potential on the beam type specimens with diverse anodes by different environments

5.2 Results of measuring cathodic protection potential

Figure 5.3 shows the cathodic protection potential curve of beam type specimens. Constant Voltage Mode was applied for the measurement to maintain output voltage for the power supplier. When setting the output voltage to 2.0 V during the test, the cathodic protection potential was not affected crucially by the experimental environment such as atmosphere, fresh water, 3% NaCl solution and kind of insoluble anodes. Moreover, the cathodic protection potential was in the range $-1,200$ to $-1,300$ mV/SSCE. As shown in Figure 5.3, the cathodic protection efficiency was good to protect the concrete structure in all experimental environments regardless of the anode such as Ti-Rod, Ti-Ribbon and Ti-Mesh.



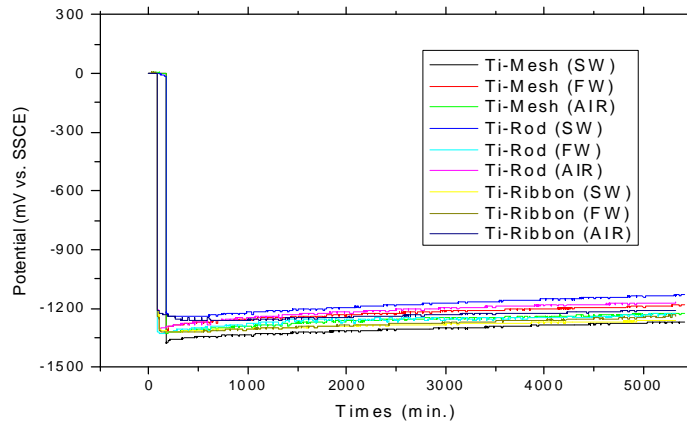


Figure 5.3 The cathodic protection potential in experimental environments



5.3 Results of measuring depolarization potential on the beam type specimens

Figure 5.4 ~ 5.6 show the behavior of depolarization. The specimens of beam type were been protecting by ICCP. When cutting off the power supply instantly, however, the potential of the specimens returned to the corrosion potential naturally. It is called the depolarization.

The potential change of specimen applied by ICCP with Ti-Ribbon anode was shown in Figure 5.4. Figure 5.5 shows the potential change of specimens used by ICCP with Ti-Rod anode. Figure 5.6 indicates the potential change of specimens utilized by ICCP with Ti-Mesh anode.

The variation of cathodic protection potential for the beam type specimen was investigated in accordance with the corrosive environments such as atmosphere, fresh water and 3% NaCl solution.

When shutting off the power supply temporarily, the ohmic resistance represented that its value was the highest in atmosphere because the concrete resistivity was the highest. On the other hand, in 3% NaCl solution, it was the lowest.

The real degree of depolarization except the ohmic resistance is 490 ~ 500 mV in sea water, 450 ~ 490 mV in fresh water and 210 ~ 220 mV in air. Besides, the value of depolarization was higher in corrosive environment than that in less corrosive environment. This is because the value of concrete resistivity in the atmosphere is higher than those in the fresh water and in the sea water.

It was found through this study that the results satisfied the standard of cathodic protection potential by NACE depending on all corrosive environment and the type of anodes for ICCP. In addition, although any

anode of different type was used for the reinforced concrete structure, the similar cathodic protection effect was presented respectively. Thus, if it is impossible to install the certain anode in the complicated concrete structure, it would be able to use the anode because of being installed easily and then it gives a opportunity to carry out the corrosion protection properly.



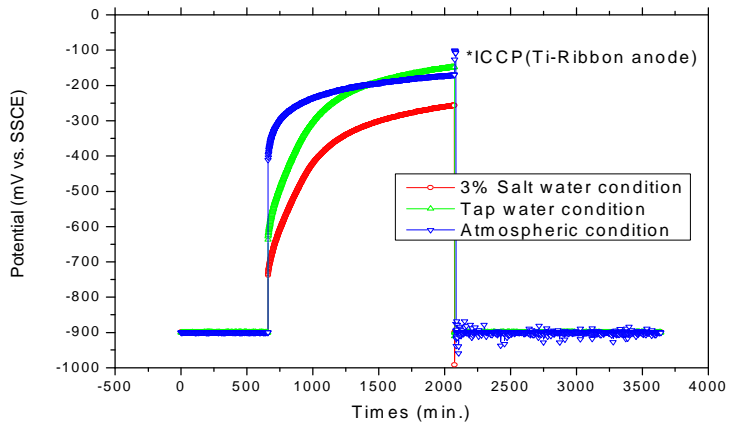


Figure 5.4 Potential shift variation of beam specimen with Ti-Ribbon anode during an instant-off measurement of ohmic interference

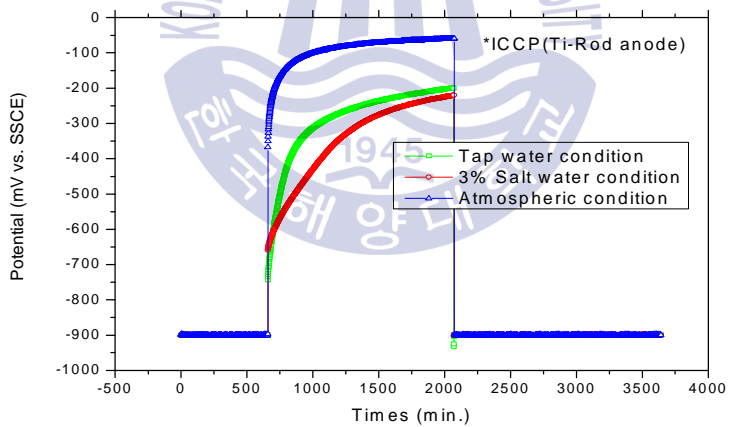


Figure 5.5 Potential shift variation of beam specimen with Ti-Rod anode during an instant-off measurement of ohmic interference

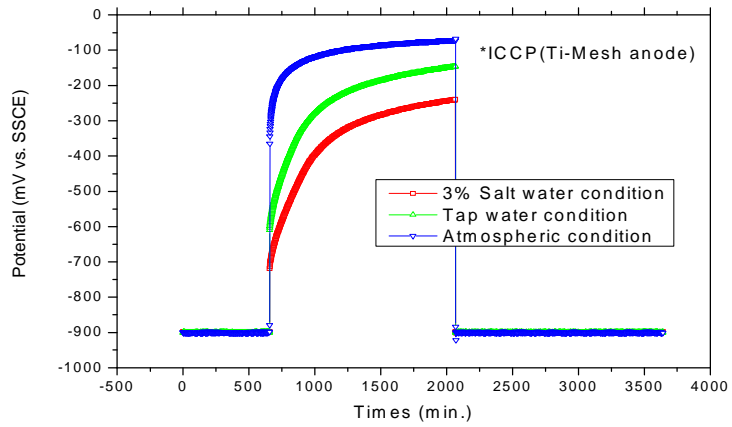


Figure 5.6 Potential shift variation of beam specimen with Ti-Mesh anode during an instant-off measurement of ohmic interference



5.4 Results of measuring depolarization potential on the slab type specimens

After being fixed the setting value of cathodic protection potential to -600 mV/SSCE by CR-1212, the depolarization test on the slab type specimens was carried out. the results are seen in Figure 5.7.

Ti-Ribbon anode was installed on the end of steel(S1) in the slab type specimens. Besides, the reference electrodes were installed the closest surface nearby each steels(S1 ~ S6). The cathodic protection potential of S1 initially maintained to -600 mV/SSCE because Ti-Ribbon anode had been installed near S1 and its set point was -600 mV/SSCE. And then those of S2 and S3 maintained to about -520 mV/SSCE. Those of S4, S5 and S6 is -470 mV/SSCE, -420 mV/SSCE and -370 mV/SSCE respectively. That is, as the distance was farther from the anode of ICCP to the cathode such as rebar in specimen, the cathodic protection potential was dropped less than the set point -600 mV/SSCE.

Briefly, the distance of between steels in the specimen was 60mm and then each of the cathodic protection potential was not dropped to the set point totally. the gap of those values was 50 mV/SSCE per 60 mm from the anode for ICCP.

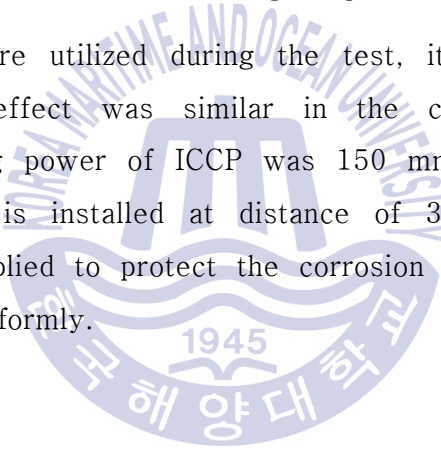
After powering off the cathodic protection system temporarily, the degree of depolarization was measured each of steels in the specimen. As the distance was farther from the anode of ICCP to the cathode such as rebar in specimen, the degree of depolarization on each steel was smaller depending on it.

Figure 5.8 represents the results of corrosion protection potential on the specimen after adding Ti-Rod anode on the S6 position.

The protection potential maintained to -530 mV/SSCE whose value is similar to setting value of CR-1212. Besides, the degree of depolarization also kept above -500 mV/SSCE after shutting off the power supply. Thus, it is a proper protection condition.

The change of cathodic protection potential by the anodes for ICCP was shown in Figure 5.9. The anodes which were composed Ti-Ribbon and Ti-Mesh were used together in Figure 5.9. The protection potential of the six steels(S1 ~ S6) has different values between $10 \sim 50$ mV. However, these were in range $-540 \sim -600$ mV/SSCE. Besides, the depolarization potential was above 500 mV and it is a good protection condition.

As any anodes were utilized during the test, it was found that the cathodic protection effect was similar in the concrete structure. In addition, the throwing power of ICCP was 150 mm from the anode for ICCP. If the anode is installed at distance of 300 mm, the cathodic protection can be applied to protect the corrosion of complex reinforced concrete structure uniformly.



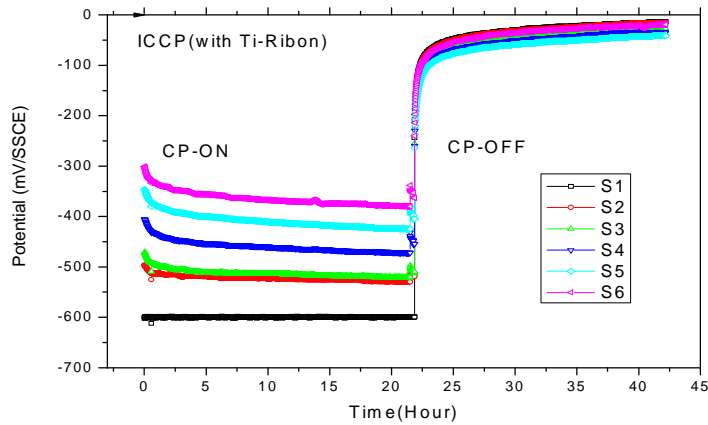


Figure 5.7 Potential shift variation of slab specimen with a Ti-Ribbon anode during an instant-off measurement of ohmic interference at 3% salt water condition

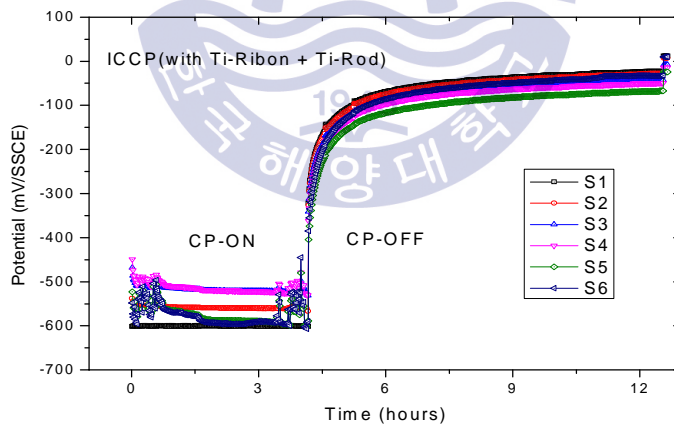


Figure 5.8 Potential shift variation of slab specimen with a Ti-Ribbon anode and a Ti-Rod anode during an instant-off measurement of ohmic interference at 3% salt water condition

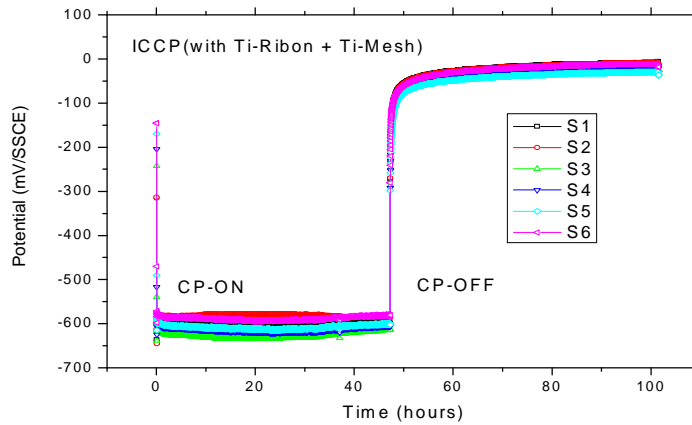
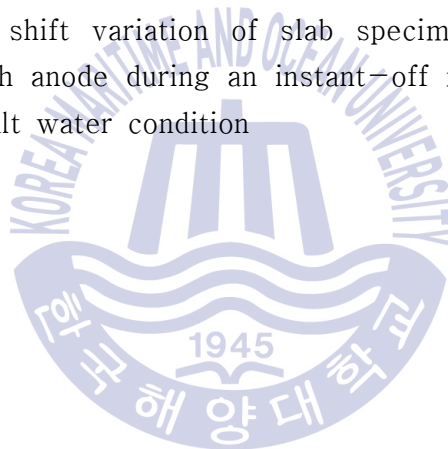


Figure 5.9 Potential shift variation of slab specimen with a Ti-Ribbon anode and a Ti-Mesh anode during an instant-off measurement of ohmic interference at 3% salt water condition



5.5 Results of measuring the cathodic protection current

Constant Potential Mode on the power supply was applied to measure the current which is used to maintain the protection potential on the specimens constantly. Besides, the setting potential value of power supply was -900 mV/SSCE.

Figure 5.10 allows to represent the protection current of insoluble anodes after filling sea water into the container on the specimens. As shown in Figure 5.10, the protection current value was initially increased after applying ICCP, but it was gradually decreased with time. Moreover, the protection current was indicated about $1.6 \sim 2.4$ mA regardless of the kind of anodes in sea water. the above current range is trivial in cathodic protection system.

Figure 5.11 shows the trend of protection current in fresh water. In fresh water environment, the protection current also was increased in accordance with time at first and then it was steadily decreased. The cathodic protection current was in the range of 1.1 to 1.6 mV.

The Figure 5.12 indicates the protection current trend of insoluble anodes in atmosphere. Through Figure 5.12, the protection current values were lower in ambient than in others environment. This is because the concrete resistivity was the highest in atmosphere. In addition, the cathodic protection current was maintained in the range of 0.6 to 0.85 mA.

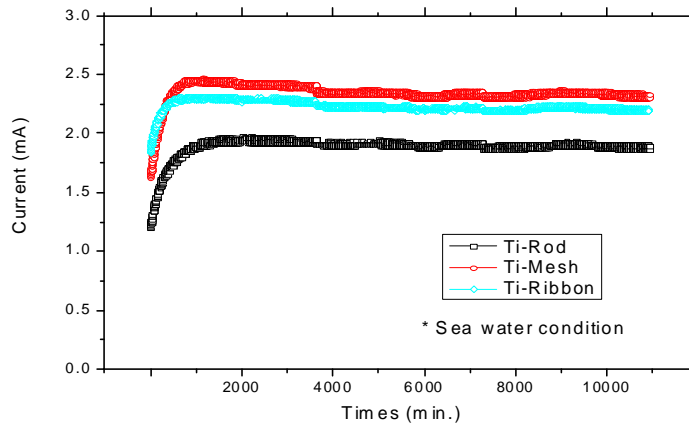


Figure 5.10 Protection current on the specimens with diverse anodes in sea water

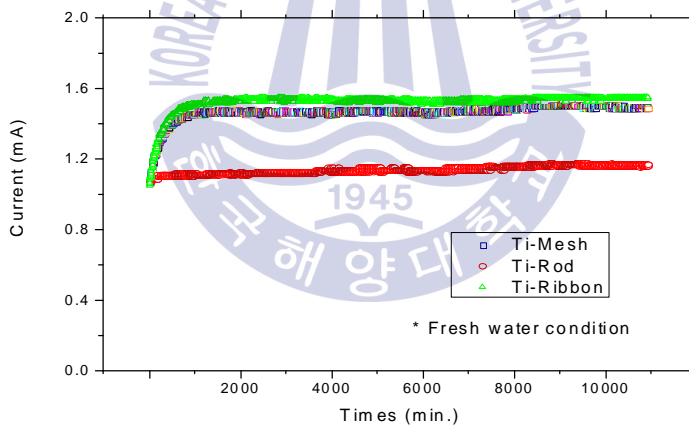


Figure 5.11 Protection current on the specimens with diverse anodes in fresh water

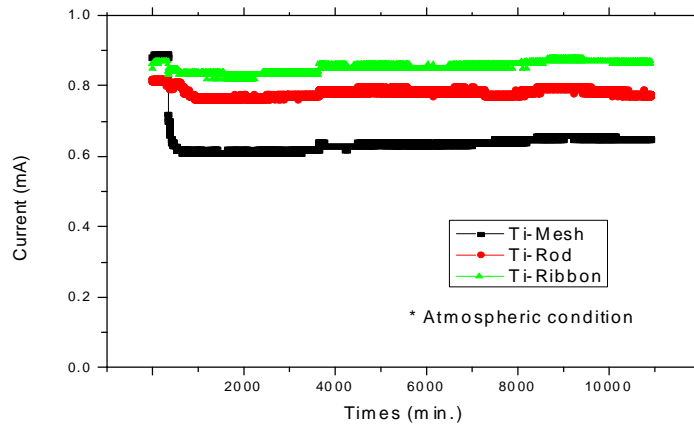
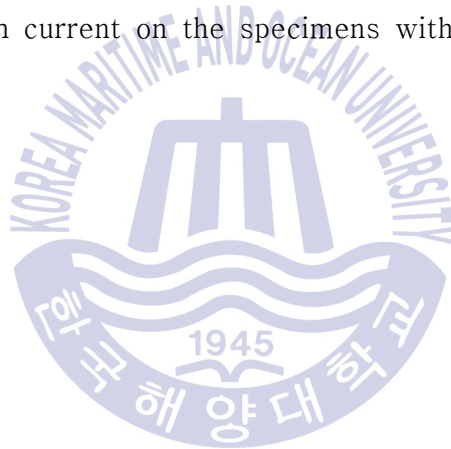


Figure 5.12 Protection current on the specimens with diverse anodes in air



Chapter 6

CONCLUSION

For this study, the anode such as Ti-Mesh, Ti-Rod and Ti-Ribbon was installed on the reinforced concrete specimen of beam and slab type. In addition, the electrochemical test was conducted to confirm the cathodic protection performance depending to the exposed environment and the kind of anode in RC structure applied with ICCP ; E-log i, cathodic protection potential, depolarization, cathodic protection current.

The following results have been obtained through the present study about the cathodic protection efficiency :

1) The E-log i test was conducted to affirm the standard of cathodic protection potential on the beam type specimen according to the environment. The standard value of cathodic protection potential was measured to about 90 ~ 140 mV. Besides, the value depending on the corrosive environment was inclined to increase slightly in order of atmosphere, fresh water and 3% NaCl solution. However, the kind of anode for ICCP nearly had no effect on the cathodic protection efficiency.

2) The cathodic protection potential was gauged by the galvanicstatic method on the beam type specimen applied with ICCP. The shape of anode had not major effect on the behavior of cathodic protection potential. In addition, the value of protection potential was tended to decrease in order of atmosphere, fresh water and 3% NaCl solution and then it was trivial difference between them.

3) The cathodic protection current was measured by the potentiostatic

method after applying with ICCP on the beam type specimen and the degree of cathodic protection current was increased by all anodes in order of atmosphere, fresh water and 3% NaCl solution.

4) The degree of depolarization was investigated on beam type specimen. The IR-Drop was the highest in atmosphere because of the concrete resistivity. On the other hand, it was the lowest in the 3% NaCl solution. Moreover, when the corrosiveness of experimental environment was higher (more severe), the real degree of depolarization except IR-Drop was more increased by concrete resistivity.

5) The cathodic protection potential was evaluated on the slab type specimen. When the distance from the anode to the rebar (cathode) is closer, the protection potential was lower by the concrete resistivity. Additionally, the potential difference represented proportionally 50 mV per 60 mm which was the distance between rebars.

6) In protecting the slab type specimen by ICCP, as the distance between the location of rebar and the anode was farther, the concrete resistivity was increased more and then the supply of protection current was limited. However, after installing the anode at regular distance supplementarily, the unprotected rebar was enabled to protect well totally.

7) As the results of protecting the slab type specimen by ICCP, it would be able to find the maximum protection distance which is about 150 mm to the rebar from the anode. That is, the anode should be installed at interval of about 300 mm to protect the whole rebars uniformly without the unprotected area.

It was found through the above results that the shape of anode used by ICCP had insignificant effect on the protection efficiency. The protection efficiency of ICCP was changed in accordance with the spacing between

the anode and rebar, and the location of anode. So, it should consider those points throughly in designing the impressed current cathodic protection. In addition, when the proper cathodic protection is applied to the reinforced concrete structures, the enormous economic problems by the corrosion will be resolved as well as the safety for human life.



References

- [1] C. Christodoulou, G. Glass a, J. Webb, S. Austin, C. Goodier, "Assessing the long term benefits of Impressed Current Cathodic Protection", Corrosion Science, Vol. 52, pp. 2671-2679, 2010.
- [2] Prasad V. Bahekar, Sangeeta S. Gadve, "Impressed current cathodic protection of rebar in concrete using Carbon FRP laminate", Construction and Building Materials, Vol. 156, pp. 242-251, 2017.
- [3] Mochammad Syaiful Anwar, B. Sujitha, R. Vedalakshmi, "Light-weight cementitious conductive anode for impressed current cathodic protection of steel reinforced concrete application", Construction and Building Materials, Vol.71, pp. 167-180, 2014.
- [4] Guofu Qiao, Bingbing Guo, Jinping Ou, Feng Xu, Zuohua Li, "Numerical optimization of an impressed current cathodic protection system for reinforced concrete structures", Construction and Building Materials, Vol.119, pp. 260-267, 2016.
- [5] Beatriz Sanz, Jaime Planas, José M. Sancho, "Study of the loss of bond in reinforced concrete specimens with accelerated corrosion by means of push-out tests", Construction and Building Materials, Vol. 160, pp. 598-609, 2018.
- [6] Xun Xi, Shangtong Yang, "Time to surface cracking and crack width of reinforced concrete structures under corrosion of multiple rebars", Construction and Building Materials, Vol. 155, pp. 114-125, 2017.

- [7] Ji-hua Zhu, Mei-ni Su, Jia-yi Huang, Tamon Ueda, Feng Xing, "The ICCP-SS technique for retrofitting reinforced concrete compressive members subjected to corrosion", *Construction and Building Materials*, Vol. 167, pp. 669-679, 2018.
- [8] Karthick Subbiah, Saraswathy Velu, Seung-Jun Kwon, Han-Seung Lee, Natarajan Rethinam b, Dong-Jin Park a "A novel in-situ corrosion monitoring electrode for reinforced concrete structures", *Electrochimica Acta*, Vol. 259, pp. 1129-1144, 2018.
- [9] Binbin Zhou, Xianglin Gu, Hongyuan Guo, Weiping Zhang, Qinghua Huang, "Durability of Innovative Construction Materials and Structures Polarization behavior of activated reinforcing steel bars in concrete under chloride environments", *Construction and Building Materials*, Vol. 164, pp. 877-887, 2018.
- [10] F.J. Luna Molina, M.C. Alonso Alonso, M. Sánchez Moreno, R. Jarabo Centenero, "Corrosion protection of galvanized rebars in ternary binder concrete exposed to chloride penetration", *Construction and Building Materials*, Vol. 156, pp. 468-475, 2017.
- [11] S.H. Xing a,b,n, Y.Li a, H.Q.Song b, Y.G.Yan b, M.X.Sun b , "Optimization the quantity, locations and output currents of anodes to improve cathodic protection effect of semi-submersible crane vessel", *Ocean Engineering*, Vol.113, pp. 144-150, 2016.
- [12] Keir Wilson, Mohammed Jawed, Vitalis Ngala, "The selection and use of cathodic protection systems for the repair of reinforced concrete structures"*Construction and Building Materials*, Vol. 39, pp. 19-25, 2013.

- [13] J. Carmona Calero, M.A. Climent Llorca, P. Garcés Terradillos, "Influence of different ways of chloride contamination on the efficiency of cathodic protection applied on structural reinforced concrete elements", *Journal of Electroanalytical Chemistry*, Vol. 793, pp. 8-17, 2017.
- [14] Elena Redaelli, Federica Lollini, Luca Bertolini, "Throwing power of localised anodes for the cathodic protection of slender carbonated concrete elements in atmospheric conditions", *Construction and Building Materials*, Vol. 39, pp. 95-104, 2013.
- [15] Jing Xu, Wu Yao, "Current distribution in reinforced concrete cathodic protection system with conductive mortar overlay anode", *Construction and Building Materials*, Vol. 23, pp. 2220-2226, 2009.
- [16] Oladis Troco' nis de Rincón, Yolanda Hernández-Lo'pez, Ange'lica de Valle-Moreno, Andre's A. Torres-Acosta, Freddy Barrios, Pablo Montero, Patricia Oidor-Salinas, Jose' Rodriguez Montero, "Environmental influence on point anodes performance in reinforced concrete", *Construction and Building Materials*, Vol.22, pp. 494-03, 2008.
- [17] Luca Bertolini, Elena Redaelli, "Throwing power of cathodic prevention applied by means of sacrificial anodes to partially submerged marine reinforced concrete piles : Results of numerical simulations", *Corrosion Science*, Vol. 51, pp. 2218-230, 2009.
- [18] Mitsumasa Iwata, Yi Huang, Yukio Fujimoto, "Application of BEM to design of the Impressed Current Cathodic Protection system for Ship Hull", *Journal of the Society of Nava Architects of Japan*, Vol. 1992, Issue 171, 1992.
- [19] L.Y. Xu, X. Su, Y.F. Cheng, "Effect of alternating current on cathodic protection on pipelines", *Corrosion Science* Vol. 66, pp. 263-268, 2013.

- [20] Moe M.S. Cheung, Chong Cao, "Application of cathodic protection for controlling macrocell corrosion in chloride contaminated RC structures", *Construction and Building Materials*, Vol. 45, pp. 199–207, 2013.
- [21] Ph. Refait, M. Jeannin, R. Sabot, H. Antony, S. Pineau, "Corrosion and cathodic protection of carbon steel in the tidal zone: Products, mechanisms and kinetics", *Corrosion Science* Vol. 90, pp. 375–382, 2015.
- [22] Yong–Sang Kim, Jeongguk Kim, Dooho Choi, Jae–Yong Lim, Jung–Gu Kim, "Optimizing the sacrificial anode cathodic protection of the rail canal structure in seawater using the boundary element method, *Engineering Analysis with Boundary Elements*", Vol. 77, pp. 36–48, 2017.
- [23] M. Narozny, K. Zakowski, K. Darowicki, "Method of sacrificial anode transistor–driving in cathodic protection system", *Corrosion Science*, Vol. 88, pp. 275–279, 2014.
- [24] G.T. Parthiban, Thirumalai Parthiban, R. Ravi, V. Saraswathy, N. Palaniswamy, V. Sivan, "Cathodic protection of steel in concrete using magnesium alloy anode", *Corrosion Science*, Vol. 50, pp. 3329–3335, 2008.
- [25] Luca Bertolini, Matteo Gastaldi, MariaPia Pedefferri, Elena Redaelli, "Prevention of steel corrosion in concrete exposed to seawater with submerged sacrificial anodes", *Corrosion Science*, Vol. 44, pp. 1497–1513, 2002.
- [26] A.A. Sag€ ues, M.A. Pech–Canul, A.K.M. Shahid Al–Mansur, "Corrosion macrocell behavior of reinforcing steel in partially submerged concrete columns", *Corrosion Science*, Vol. 45, pp. 7–32, 2003.
- [27] Denny A. Jones, "Principles and Prevention of Corrosion", 2nd Edition, Prentice Hall, pp.1–165, 1996.

- [28] J. P. Broomfield, " Corrosion of Steel in Concrete", 2nd Edition, Taylor & Francis, pp.1-2, 2007.
- [29] Gerhardus H. Koch et al, "Corrosion Costs and Preventive Strategies in the United States", NACE, FHWA-RD-01-156, 2002.
- [30] "Leo Frigo Memorial Bridge failure", NACE, www.nace.org/Corrosion-Failure-Leo-Frigo-Memorial-Bridge-Failure.aspx.
- [31] " Lowe's speedway bridge collapse", NACE, www.nace.org/CORROSION-FAILURES-Lowes-Motor-Speedway-Bridge-Collapse.aspx.

